

**Non-linear mixed effect models for mechanical trials of
biomaterials**

André Filipe Martins Abreu

Thesis to obtain the Master of Science Degree in

Mechanical Engineering

Supervisors: Prof. Susana de Almeida Mendes Vinga Martins
Prof. Pedro Alexandre Lopes de Sousa Martins

Examination Committee

Chairperson: Prof. Paulo Jorge Coelho Ramalho Oliveira
Supervisor: Prof. Susana de Almeida Mendes Vinga Martins
Member of the Committee: Prof. João Orlando Marques Gameiro Folgado

November 2017

Acknowledgments

Firstly, I would like to thank to Prof. Susana Vinga and to Prof. Pedro Martins for the inspiring teaching and all the support that they gave throughout this work. Their knowledge and comprehension over the unforeseen were very encouraging. To the project NEMESIS(LAETA) that was indispensable for the conclusion of this thesis. Finally, to my friends, especially Catarina Gonçalves, Miguel Faustino, Marisa Lima, Rodrigo Gonçalves and João Franguito, I leave a big thanks for the help through the all course. Lastly, I would like to thank to my family for their support at all times during my academic path.

Resumo

O Prolapso dos órgãos pélvicos é uma doença que aflige mulheres de todas as idades, afectando severamente a sua qualidade de vida. Esta condição é caracterizada pela descida dos órgãos intra-pélvicos. Seguindo o interesse crescente da comunidade científica neste tópico, este estudo pretende descrever as propriedades mecânicas do tecido vaginal, um dos órgãos mais afectados. Visando o objetivo proposto, nós implementámos um modelo não-linear de efeitos mistos para modelar as dinâmicas presentes nos testes de tracção de tensão uniaxial aplicados a amostras de tecido vaginal. Onde a predição da tensão como dependencia do alongamento é uma proposta inovativa. Também é explorado a possibilidade de implementar o modelo usando atributos facéis de obter. Esta tese recorreu a uma base de dados de ensaios biomecanicos às amostras de tecido e às características de cada paciente. Neste estudo demonstrámos que existe uma correlação entre as variáveis de cada paciente e as propriedades mecânicas dos seus tecidos. De acordo com os resultados obtidos, em media, a idade e o numero de partos naturais estão associados a um aumento da tensão maxima registada nos testes. Nesta tese, também, é proposto um algoritmo iterativo para identificar e remover observações discrepantes. Quando aplicado à base de dados analisada, este método permitiu uma diminuição do erro e dos efeitos aleatórios em 11% e 45%, respectivamente, com a exclusão de 17% das amostras. Este procedimento inovador ganha maior destaque, sabendo que pode ser facilmente aplicado a todas as áreas onde os modelos NLME já provaram ser relevantes. Os resultados obtidos estabelecem uma base sólida para se inferir com mais precisão que variáveis podem estar associadas ao comportamento mecânico dos tecidos humanos. A aplicação das abordagens propostas a outras bases de dados poderá potenciar o desenvolvimento de novos meios de diagnóstico e de tratamento.

Palavras-chave: modelo não-linear de efeitos mistos, efeitos aleatórios, tecido vaginal, observações discrepantes, Prolapso

Abstract

Pelvic organ prolapse (POP) is a disorder that afflicts women of all ages, severely affecting their life quality. This condition can be characterized by the drop of intrapelvic organs. Following the growing interest of scientific community in this issue, this study intends to describe the mechanical behavior of vaginal tissue, which is one of the organs most affected. For this purpose, we implemented a nonlinear mixed effect (NLME) model to study the dynamics present in the uniaxial tensile tests performed on vaginal tissues. Where the prediction of the stress as a dependency of stretch is an innovative proposal. We also explore the possibility of implementing the model using attributes that are easily obtained. This thesis resorted to a database of the results of several experiments applied to tissue samples and patients co-variables. Here we show that a correlation exists between the patients' co-variables and the mechanical properties of their tissues. According to results obtained, on average, the age and the number of children are associated with an increment of the maximum stress registered in the tests. In this thesis, we also proposed an iterative process to identify and remove outliers. When applied to our dataset, this process reduced the error and variance of the random effects by 11% and 45%, respectively with an exclusion of 17% of the samples. This innovative method has further relevance since it can be easily applied to all areas where the NLME models are proved to be useful. The application of the suggested approaches to other databases could help the development of new means of diagnosis and treatment.

Keywords: NLME, POP, Random effects, Vaginal tissue, Outliers

Contents

Acknowledgments	iii
Resumo	v
Abstract	vii
List of Tables	xi
List of Figures	xiii
Nomenclature	xv
Glossary	1
1 Introduction	1
1.1 Motivation	1
1.2 Objectives	2
1.3 Thesis Outline	2
2 Medical and mechanical context of prolapsed tissue	3
2.1 Pelvic organ prolapse overview	3
2.1.1 Pelvic organ prolapse	4
2.1.2 Vaginal wall tissue	4
2.2 Mechanical properties evaluation of soft tissues	5
2.3 Technical procedure to evaluate tissues	8
3 Model and algorithms	11
3.1 Nonlinear mixed-effects models	11
3.1.1 Nonlinear mixed-effect models as a hierarchical model	12
3.1.2 Model mathematical introduction	13
3.1.3 Model Contextualization	14
3.2 Outliers detection in time series	17
3.3 Levenberg-Marquardt algorithm	20
4 Implementation	23
4.1 Program generic flowchart	23
4.1.1 Data processing	24
4.1.2 Fitting observations	25

4.1.3	Fitting covariables	26
4.1.4	Create a Nonlinear mixed effects model	27
4.2	Iterative process to remove outliers	28
5	Datasets description	33
5.1	Artificial data	33
5.2	Real data analysis	37
6	Model results	41
6.1	Artificial data	41
6.2	Real data	44
7	Conclusions	55
7.1	Future Work	56
	Bibliography	59
A	Results tables	63

List of Tables

5.1	Patients and their co-variables present in the dataset.	39
5.2	Statistical description of the patient co-variables.	39
5.3	Statistical description of the samples fittings	39
6.1	Correlation matrix between patients co-variables and fittings parameters	45
6.2	Statistical description of samples fittings.	46
6.3	Analysis of the fittings quality per sample	46
6.4	Analysis of the fittings quality per patient	46
6.5	Outliers identified	49
6.6	Statistical analysis of the initial model and the final model	51
6.7	Statistical analysis of the simple model and the final model	52
A.1	Sample properties	63
A.1	Sample properties	64
A.1	Sample properties	65
A.2	Fittings results of the real data Patients	66
A.3	Fittings results of the real data samples	66
A.3	Fittings results of the real data samples	67
A.3	Fittings results of the real data samples	68
A.3	Fittings results of the real data samples	69

List of Figures

2.1	(A) Relation of the anterior and posterior vaginal wall; (B) 'H' shaped on cross-section (Source: [14])	5
2.2	Vaginal layers (Source: https://o.quizlet.com/DmqtuuBm.1.Jwg3YLo9q-w.jpg)	5
2.3	Uniaxial tension test for assessment of biomechanical properties of vaginal tissue. The reference configuration (F_1, L_0, A_0) is changed during the mechanical test $(F_2, L_0, A_1$ and $\Delta L)$. (Adapted from [19][20])	6
2.4	Stress (σ)-stretch (λ) curve showing the stiffness and maximum stress. Stiffness is the slope of the linear portion of the curve. (Adapted from [19])	7
2.5	Preconditioning of an anterior cruciate ligament. Each cycle shows evidence of hysteresis. (source:[20])	7
2.6	Prolapsed vaginal tissue from one patient (Adapted from [20])	9
2.7	Sample preparation. (d) Mounting the sample in the test rig. (Adapted from [20])	9
3.1	Multilevel perspective of a hierarchical model.	12
3.2	Stress(σ)-stretch(λ) curve of a patient's sample.	14
3.3	Fittings using the three proposed equations applied to a Patient sample.	15
3.4	Example of the three outlier types proposed.	19
4.1	Simplified model of program flowchart.	24
4.2	Detailed view of data treatment block.	24
4.3	Detailed view of $f(\cdot)$ fitting block.	25
4.4	Detailed view of $d(\cdot)$ fitting block.	26
4.5	Detailed view of model creation block.	27
4.6	Information diagram of command <i>nlmefit</i>	28
4.7	Iterative process flow chart	29
4.8	Flow chart of Iterative process implemented to identify e exclude outliers	30
5.1	Co-variables generated in an example dataset	35
5.2	Three generated samples of one patient	37
5.3	Variables transformation	38
5.4	Tests on samples from the same patient	40

6.1	Influence of noise added to the samples on the model results. Parameters $dv = 0.7$ and $P_{Out} = 10\%$.	42
6.2	Three generated samples of one patient	43
6.3	Three generated samples of one patient	43
6.4	Relation between patients co-variables and estimated c_1	45
6.5	Relation between patients co-variables and estimated c_2	45
6.6	Relation between patients co-variables and estimated c_3	45
6.7	Example of two with a high inter-individual variability	47
6.8	Variation of the random effects variance with the number of outliers removed.	48
6.9	Variation of the model RMSE with the number of outliers removed.	48
6.10	Samples of the Patient 31.	49
6.11	Example of an outliers removed by the algorithm.	50
6.12	Comparing the predicted values with the real values.	50
6.13	Residuals from the non-linear fit.	51
6.14	Influence of the Age on the predicted uniaxial tensile tests. Both samples have $NVB = 3$ and $YM = 15.5$.	53
6.15	Influence of the YM on the predicted uniaxial tensile tests. Both samples have $NVB = 3$ and $Age = 63.6$.	53
6.16	Influence of the NVB on the predicted uniaxial tensile tests. Both samples have $YM = 15.5$ and $Age = 63.6$.	54

Roman symbols [ru]

Greek symbols [g]

Subscripts [s]

Chapter 1

Introduction

1.1 Motivation

Pelvic organ prolapse (POP) is a common, non-life-threatening condition-affecting woman of all ages [1]. Although the mortality associated with these disorders is low, the quality of life and perception of the patient's own body are severely affected [2].

The exact percentage of the population that suffer of such disease is unknown, but recent studies estimated that 25% of adult women in the United States have more than one pelvic floor disorder, and 1 in 4 women will undergo surgery for stress urinary incontinence or pelvic organ prolapse during their lifetime. Routine gynecological examinations reveal evidence of pelvic organ prolapse in up to 50% of adult women [3]. Other studies made in Australia and Sweden, have been performed on the prevalence of POP in a general population. One of them, using a postal questionnaire, symptomatic POP was found in 4-12.2% of all women. In the United States alone, the costs for POP and incontinence surgeries are more than \$1 billion per year. Unfortunately, this number is expected to double in the next 30 years, as a result of the increasing age and the changes into the lifestyle that will be reflected in the number of women that resorts to the healthcare system [4]. To aggravate this situation, incidence peak of surgery for pelvic organ prolapse is in individuals of age between 60–69 years and is estimated that 13% of patients who have surgery will need to repeat the operation within the following five years [5].

Despite the number of reports devoted to investigating these diseases being steadily increasing, there is a paucity of epidemiological studies of the natural history of pelvic disorders, making it difficult to understand their pathophysiology deeply [2]. Reliable models can be useful tools to perform objective and specific evaluation of pelvis [6]. Hence, identify the impact of different surgical treatments and determine the most precise ways of preventing the disease is the fundamental motivation of the present work.

1.2 Objectives

To help minimize the lack of knowledge about the topic under study, the work described in this document has several objectives:

1. Predict the stress/stretch curve accurately on a uniaxial tension test of vaginal tissue using a Non-linear mixed-effects models;
2. Among the features available in the dataset, identify the most relevant for the study of mechanical behavior of the vaginal tissues;
3. Conclude which dataset features positively influence the model accuracy;
4. Evaluate how the model error changes when a process of outliers detection is implemented;
5. Develop a NLME model automatically and apply methods to improve its accuracy;
6. Explore the possibility of applying this thesis's approach to other human tissues.

These work objectives require a previous analysis of the patients' features and understanding of how they correlate with the equation parameters used to make the fitting of Stress/Stretch curve of each patient.

1.3 Thesis Outline

In **Chapter 2**, the fundamental biomechanics background that supports this work. An overview of POP disorder and an explanation of the mechanical properties of the human tissues will be presented.

The fundamental concepts of Nonlinear mixed-effects models applied to our problem and the theory behind optimization algorithms used to infer the proposed approach are described by the **Chapter 3**.

In **Chapter 4**, the process of creating the Nonlinear Mixed-effect models based on the uniaxial tensile test data and the iterative process to exclude outliers are explained.

The **Chapter 5** is dedicated to described the datasets used to develop NLME models. The implementation of the real dataset follows the collaboration of several entities as part of the project NEMESIS. In this scope, the University of Porto supplied us the information regarding the biomechanical tests of patient's vaginal tissues.

In **Chapter 4**, the results obtained applied to the dataset will be presented. Based on the results obtained this study will be able to conclude in what degree the objectives proposed were achieved.

Conclusions about the model ability to describe the biomechanical tests of vaginal tissue is discussed in **Chapter 6**. The proposed method of outliers detection is also discussed. The last chapter includes some notes on the future work to improve the developed approach.

Chapter 2

Medical and mechanical context of prolapsed tissue

The present chapter addresses the fundamental biomechanics background that supports this work. An overview of POP disorder and an explanation of the mechanical properties of the human tissues will be presented in the following sections.

To accomplish the proposed objectives, we had to investigate the effects of POP in the damaged tissues and the repercussions in their mechanical properties. The ability to represent all the mechanical dynamics mathematically is the key factor that will determine the quality of the present work results.

The relevance of POP in the world nowadays will be explained and how it will change in the future. Several studies have been developed regarding this problematic. They proved that the disease is widespread across the women population and it tends to increase its prevalence.

POP influences all the pelvic system, but we will focus on the vaginal tissue. The dataset that we will use is related to this human organ. Hence, is crucial that we describe the vagina in detail and how it can be influenced.

This work rely on the past work developed by numerous authors that described a general mechanical behavior for human tissues. Its characterization is the basis of the models implemented.

This study was not responsible for gathering the data. Therefore, we will show the general procedures to collect and test the tissues, but it will not be the primary focus of this thesis.

2.1 Pelvic organ prolapse overview

The current session is devoted to describing the disorder under study. This explanation is essential to implement the model and understand its results.

2.1.1 Pelvic organ prolapse

Several reports characterize this disease as the drop of intrapelvic organs such as the uterus, bladder, urethra and rectum. Deficiencies in the pelvic support system are the cause of this disorder [7]. Which, most of the times, is characterized by a sensation of a bulge or protrusion, seeing or feeling a bulge or protrusion, pressure and heaviness [5]. There are several health problems associated with POP. Urinary incontinence (UI) and stress urinary incontinence are counted among the most common [8].

In the literature, several studies indicate that POP is a multi-factorial problem. Vaginal birth is presumed to be one of the most relevant risk factors especially if forceps were used [9]. The risk of having prolapse surgery was more than doubled after forceps delivery compared with both vacuum and non-instrumental delivery, and more than 20 times that of cesarean [10]. Age is considered to be the only non-modifiable risk factor that is inherently and directly related to the incidence of POP. According to published reports, POP occurs mostly in older women, where the average age of patients with prolapse is 62 years old. Furthermore, the associated risk of developing POP becomes higher every year [2]. Women that are submitted to a gynecologic surgery, especially hysterectomy, are more predisposed to develop prolapse. In another context, some evidences show that menopausal women who took standard doses of hormone or estrogen replacement for 5 or more years were less likely to develop pelvic floor disorders [11]. Previous studies found a substantially increased risk of surgery for pelvic floor disorders among first-degree female relatives of operated women. Hamer and colleagues supported the theory that there is a heredity component in the development of genital prolapse [12]. Increasing body-mass index also seems to have a role in the development of pelvic organ prolapse. Women who are overweight (body-mass index 25–30 kg/m²) and obese (30 kg/m²) are at higher risk of developing this disorder [5]. The race is another common risk factor described in the literature. Previous research documents that there is a greater incidence of POP in white women, compared with black women [4][9].

2.1.2 Vaginal wall tissue

In order to easily understand this vaginal disorder, it is to have in mind the structural component of the this organ.

The vagina is a flat fibromuscular tube whose anterior and posterior walls are collapsed onto each other, extending from introitus to fornices that surround the cervix [13].

The walls of the vagina are usually in close contact, except at the upper end where the cervix projects into the vagina. Because of the position of the cervix, the anterior wall of the mature vagina measures around 7.5 cm, and the posterior wall approximately 9 cm [15].

The vaginal wall is usually divided in three tissue layers: mucosa, muscularis and adventia [16]. Mucosa layer corresponds to approximately 20-25% of the total thickness of vaginal wall [17, 18]. The vaginal mucosa is divided into two parts: epithelium and the underlying lamina propria. Epithelium consists of basal, parabasal, intermediate and superficial squamous cells responsive to hormonal stimuli. Smooth muscle, small blood vessels, capillaries, and nervous tissue are situated in the lamina propria, which is principally composed of connective tissue. The muscular layer consists primarily of smooth muscle

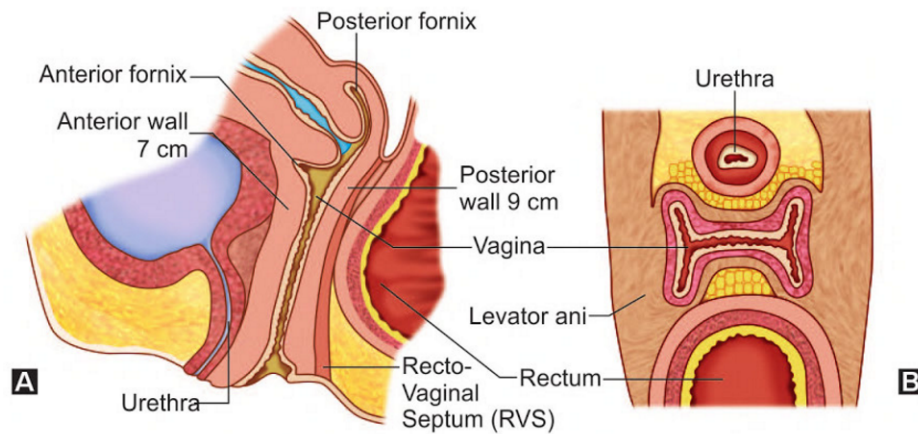


Figure 2.1: (A) Relation of the anterior and posterior vaginal wall; (B) 'H' shaped on cross-section (Source: [14])

with bundles of circular fibers internal to longitudinal fibers. Finally, the last coat, adventitia is a variable discrete connective-tissue layer of collagen and elastin between the muscular wall of the vagina and the adjacent paravaginal connective tissue.

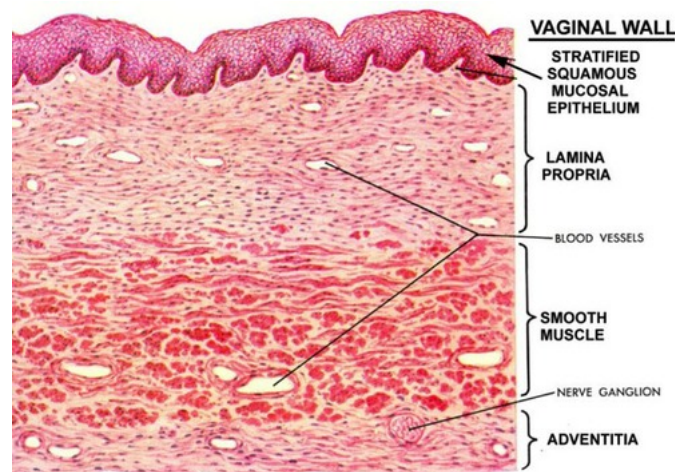


Figure 2.2: Vaginal layers (Source:<https://o.quizlet.com/DmqtuuBm.1.Jwg3YLo9q-w.jpg>)

2.2 Mechanical properties evaluation of soft tissues

The definition of the biomechanical properties of vaginal tissue is an essential step in the modeling of the pelvic cavity, which is required to understand the physiopathology of prolapse [6]. Therefore uniaxial tension test becomes a very valuable tool to describe the disease and to understand what variables influence the degradation of tissue.

In a uniaxial tension test, the quantities measured are the force applied, F , the elongation of the gauge, ΔL and the cross-sectional area, ΔA .

As reported by Martins [20] the techniques used to measure typical engineering materials, such as, metals and composites, cannot be applied to biologic tissues. Their high deformation characteristic

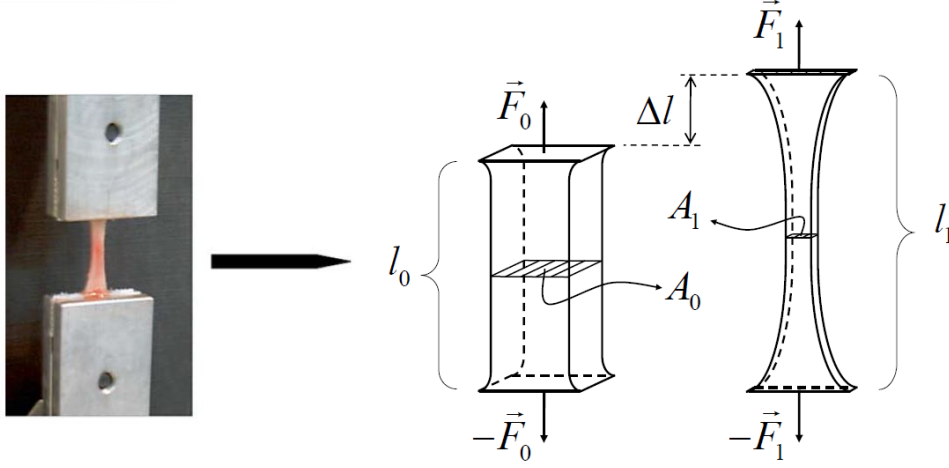


Figure 2.3: Uniaxial tension test for assessment of biomechanical properties of vaginal tissue. The reference configuration (F_1, L_0, A_0) is changed during the mechanical test (F_2, L_0, A_1) and ΔL . (Adapted from [19][20])

affects the cross-section measurement. It is also reported that there is several methods of measure the geometric deformation for highly deformable materials such as, digital image correlation (DIC) and video extensometry (VC). The Figure 2.3 shows the geometrical properties that should be measure in this type of tests.

Generally in the literature, due to simplification purposes, this type of materials are considered incompressible. Therefore we are able to apply the equation of volume preservation during the test. Which can be described as:

$$V_0 = V_1 \Leftrightarrow A_0 \cdot l_0 = A_1 \cdot l_1 \quad (2.1)$$

Data is then manipulated in order to take into account the sample geometry. The elongation measurement is used to calculate the engineering stretch λ :

$$\lambda = \frac{l_0 + \Delta l}{L_0} \quad (2.2)$$

To achieve the engineering stress, σ , we employ the force measurement, resorting to the following equation:

$$\sigma = \frac{F}{A} \quad (2.3)$$

According to Martins and colleagues [19], vaginal tissue, as a soft tissue, displays non-linear mechanical behavior when subjected to uniaxial tension tests. In this context, the term non-linear describes the mathematical function providing the relation between stress σ and the stretch λ i.e., $\sigma = f(\lambda)$.

As can be seen in Figure 2.4, the typical mechanical behavior of vaginal tissue has three main regions. The region A and C are non-linear, and the middle region B is linear. In the linear part, the slope, E, represents the stiffness. The stiffness parameter, E, is also called the modulus of elasticity and is a measure of a material's resistance to elastic deformation. The S_{\max} is also known as ultimate stress and

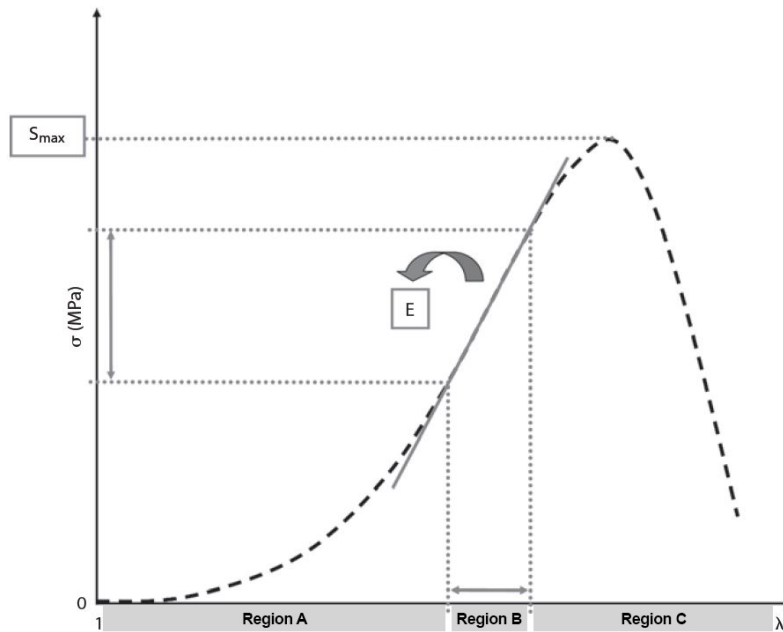


Figure 2.4: Stress (σ)-stretch (λ) curve showing the stiffness and maximum stress. Stiffness is the slope of the linear portion of the curve. (Adapted from [19])

is the maximum stress which a material will withstand before rupture.

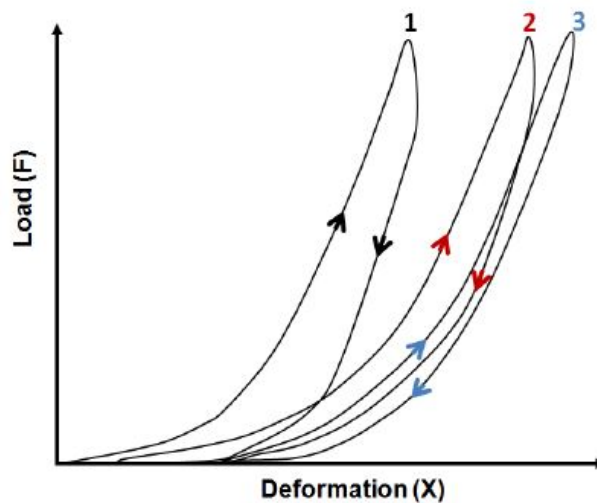


Figure 2.5: Preconditioning of an anterior cruciate ligament. Each cycle shows evidence of hysteresis. (source:[20])

When a soft biologic tissue in general, and vaginal in particular, is loaded with a simple force from its original state, unloaded and then reloaded, the stress required on reloading is less than that reached in the initial loading for stretches up to the maximum stretch achieved in the previous loading step. That can be seen in Figure 2.5, where after a load cycle, the tissue does not fully recover its original form. We referred this stress softening phenomenon as hysteresis effect. After the birth, this effect is a major factor when the vaginal tissue supports high load distribution and the tissue does not recover its original behavior [8]. In the same study, Peña et al. [8] conclude that stress softening phenomenon may be put in the broader context of the existing clinical evidences of pelvic organ prolapse being one of the

unfavorable outcomes of vaginal birth.

Material composition is a critical factor in the behavior of the Stress-stretch curve. The connective tissue of vaginal tissue contains collagen, elastic fibers and proteoglycans as predominant extracellular matrix components. Collagen contributes significantly to the biomechanical properties of the tissue since it provides resistance to stretching. Fibrillar collagens I and III are the main constituents of the extracellular matrix and are responsible for tissue structural integrity. Type I contributes to tensile strength while type III fibers provide elasticity. Changes in the amount of these components lead to a different response when the load is applied [21, 22, 23]. Kerkhof et al. [24], in their study, found a tendency toward a higher amount of collagen III relative to the stronger type I collagen in the anterior vaginal wall of patients with POP is thought to result in thinner collagen fibers with correspondingly diminished biomechanical strength.

Constitutive modeling of soft tissues has been an area of extensive research in the last few years([25, 26]). In a recent paper, Martins et al [27] modeled vaginal tissue as a hyperelastic material and led to the proposal of a strain energy function (SEF) adapted to the tissue structure. This work was followed by an investigation concerning the damage mechanisms in the tissue due to the application of stresses outside the physiological range analyzed in some mechanical test [28]. Despite the success of the developed studies, the models present three main problems:

- Do not take into account the inter and intra-patient variability of the responses;
- Models are based in non-intuitive variables;
- To have good fitting results, the models become very complex.

We propose to use NLME models to address the problems currently identified in modeling this type of curves, namely the inability to describe all the dynamics present in the uniaxial tensile tests and the predictions of the mechanical properties of the tissues fail to include the influence of the patient co-variables.

2.3 Technical procedure to evaluate tissues

To fulfill this thesis's objectives, we require a dataset that provides the information relevant for the model implementation. Knowing that our focus is on the system's mathematical description, we were not responsible for collecting the dataset. In the scope of a collaboration between the Faculties of Engineering and Medicine of the University of Porto and *Hospital de S. João do Porto*, patient's vaginal tissues were collected and submitted to mechanical tests.

The procedures are described and explained in [8], [19],[20] and [27]. In the present work, we will use the database already created with the biomechanical tests.

Experimental vaginal tissues were gathered from women submitted to surgery for POP. The study was conducted following the Ethical Research Ethics Committee guidelines of *Hospital de S. João do Porto*. Patients give their consent for the following studies. All women were previously evaluated by several

factors, such as history, physical examination and some by urodynamic study. The severity of POP symptoms was previously evaluated as well. To be admitted in the present study, women must had vaginal prolapse at least stage 2 of POP-Q [19].

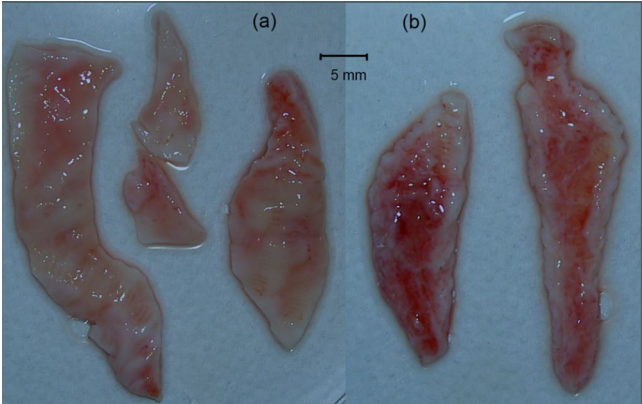


Figure 2.6: Prolapsed vaginal tissue from one patient (Adapted from [20])

Regarding the technical procedures, the prolapsed vaginal tissue was removed in the surgical procedure. Then it was frozen in a saline solution at -20 °C until 15 minutes before the start of the mechanical test. The described procedure was adopted because according to several authors, this method does not affect the mechanical properties of the samples [8].

The Figure 2.6 shows an example of a vaginal sample. Where the tissue was cut in the longitudinal axis of the middle third vagina in the anterior and posterior vaginal walls. Note that samples with visible damages such as holes and cuts were not tested.

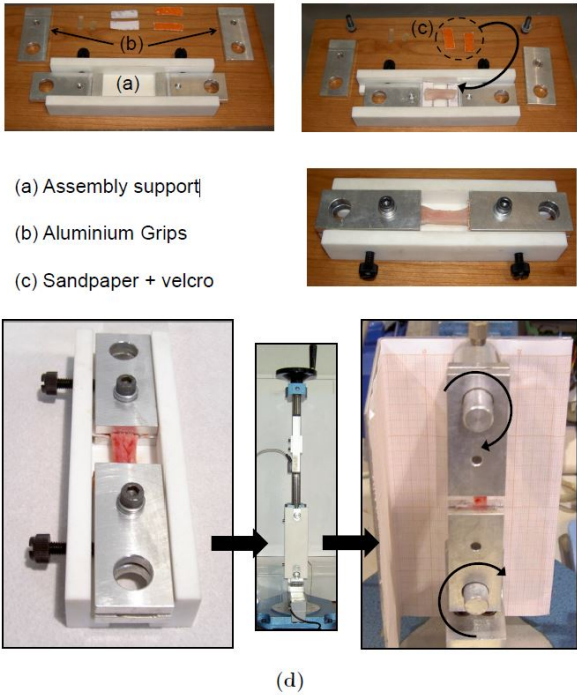


Figure 2.7: Sample preparation. (d) Mounting the sample in the test rig. (Adapted from [20])

Once removed the tissues, the mechanical tests were performed on each valid sample. Accordingly with

Martins et al. [8], the sample tissues were fixed on the testing machine utilizing an assembly support. It should be noted that the device was developed by Martins and colleagues to perform uniaxial tensile tests on soft tissues. The figure 2.7 shows the system where the sample mechanical properties are evaluated. Geometric properties were measured using a digital image analysis [19].

After gathering the data, it was applied the equations described in subsection 2.2 to transform force and elongation into stress and stretch.

Chapter 3

Model and algorithms

This chapter will present the fundamental concepts of Nonlinear mixed-effects models applied to our problem and the theory behind optimization algorithms used to infer the proposed approach.

3.1 Nonlinear mixed-effects models

Nonlinear mixed-effect modeling is mainly applied to longitudinal data. For repeated measures it can be thought of as a hierarchical model involving both fixed-effects associated with the population parameters and random-effects accounting for unexplained inter- and intra-individual variability [29].

Possible applications for this models are vast. In many time-series investigations, including those on human immunodeficiency virus (HIV) viral dynamics, pharmacokinetic reports, and studies of growth and decline analysis, it is becoming one of the most popular type of model [30]. Nowadays, they are a routine tool for the analysis of pharmacokinetic and pharmacodynamic data obtained in clinical trials during drug development [31]. In another field, M. Brabec et al. [32], faced several irregularities in the individual consumption series of natural gas posed by heterogeneity of the inter-individual observations. The irregularities include zeros, missing data, and abrupt changes of the consumption patterns. They implemented, with relative success, a nonlinear mixed effects model on those conditions. In ecology, it was used to model the effect of wind speed and crown class in the height-diameter of one tree species, lodgepole pine [33]. To ensure safety and reliability of engineering systems in nuclear plants, Yuan et al. [34] implemented a NLME model to track degradation trends and predicting its evolution with time using in-service inspection data. Lorino et al. [35] model the pavement deterioration based on repeated measurements on the same section to investigate and test the importance of climatic factor. In this article, the authors explore the possibility of using NLME models to describe relationships between the postharvest environment, such as storage conditions, fruit dry matter at harvest, and the incidence of pathological and physiological disorders in fruit after cold storage [36].

As described, the literature on NLME models shows a wide variety of applications, but to our knowledge, all the models have been developed as a function of time. This study introduces a new approach, where the purpose is to predict the stress in a uniaxial tensile test as a dependency of the stretch. Stretch,

our "time", is also continuous, monotone increasing function, and always positive. Therefore, all the keys conditions demonstrate the feasibility of this new proposal. Furthermore, it is possible to include covariates and evaluate the association between them and the resulting biomechanical properties.

In this work, we explore the possibility of implementing a NLME model using attributes that are intuitive and easy to obtain. Patient features used were only the ones described in the literature as being potential risk factors of pelvic organ prolapse. Age, menopause stage, hormonal treatments, number of natural childbirths are some examples.

3.1.1 Nonlinear mixed-effect models as a hierarchical model

A hierarchical model assumes that the data is nested in groups. Therefore, we can not analyze one sample without having in mind that it is influenced by the group where it is included. In this study, applying a hierarchical model is particularly useful because the individual characteristics influence the properties of the samples, as we explained in the previous chapter. In this context, our models are used to explore the association between individual attributes and their vaginal tissue response to a uniaxial tensile test.

Nonlinear mixed effects model, in the form of a continuous repeated measurements on each of individual, can be considered as a hierarchical model because the parameters of the statistical model vary at more than one level [37].

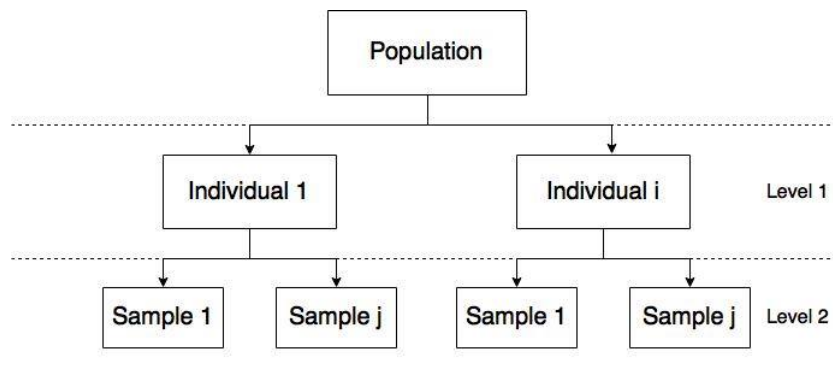


Figure 3.1: Multilevel perspective of a hierarchical model.

As can be seen from figure 3.1 the model to be implemented is composed by two levels. The first and second tier are related respectively to the inter-individual and intra-individual variations in the measurements respectively.

Working the data with this structure allows having the focus on individual-specific characteristics. In other words, this work assumes that characteristics of each have the primary influence on stress-stretch curve of the samples. Therefore, the generalization of measurements predictions of one individual to another cannot be accomplished without incurring in significant errors. Nonlinear mixed effects model incorporates the individual characteristics as fixed effects.

Even though the samples of one individual share the same individual-specific characteristics, they do not present the same measurement results. Regarding this problem, we consider several causes. As

reported by H.B. Motra et al [38], the sources of uncertainty, related to measurements methods, include configuration, number and distribution of measuring points, sampling, filtering, the definition of the measurement task, process planning, equipment handling, fixturing, as well as operator's influence. For being so difficult to represent mathematically, these variations between samples of the same individual are treated by NLME as random effects. Random effects capture the correlation between repeated measurements within a subject [39].

In conclusion, NLME models recognize correlations within sample subgroups, providing a reasonable compromise between ignoring the groups dynamics entirely, therefore losing relevant knowledge, and fitting each group independently, which requires significantly more data points.

3.1.2 Model mathematical introduction

The nonlinear mixed effects model is a natural generalization of linear mixed effects model. Let y_{ij} denote the j th measurement of the response. In this case, it represents the stress resultant for a certain value of stretch, under the condition $t_{ij}, j = 1, \dots, n_i$ and possible relevant additional conditions u_i . For simplification purposes, it will be assumed that u_i is empty, then $x_{ij} = (t_{ij}, u_i) = t_{ij}$. Each individual has a vector of their characteristics defined by a_i , which do not change over the measurements, for example, age, parity and hormonal treatments. Letting $y_i = (y_i, u_i, a_i)$ be independent across i , reflecting the belief that individuals are unrelated. The NLME model can be written into a two-stage hierarchical form as follows:

Stage 1: Intra-subject variation

$$y_{ij} = f(x_{ij}, \beta_i) + e_{ij}, \quad j = 1, \dots, n_i. \quad (3.1)$$

In equation 3.1, $f(\cdot)$ represents a function governing within-individual behavior and it depends on a $(p \times 1)$ vector of parameters, β_i , specific to the individual i . The function $f(x_{ij}, \beta_i)$ represents what happens "on average" for all possible realizations of actual response trajectory and measurement error that could arise if subject i is observed. Generally, the function f is incapable of include all the process dynamics, meaning that the real response, followed by the dotted line, is always different than the predicted output. Parameter e_{ij} represents the absolute error between the actual and the predicted response. It is commonly assumed that intra-individual deviations $e_{ij} = y_{ij} - f(x_{ij}, \beta_i)$ have mean equal to zero, $E(e_{ij} | \beta_i) = 0$.

Stage 2: Inter-subject variation

$$\beta_i = d(a_i, \beta, b_i), \quad i = 1, \dots, m, \quad (3.2)$$

Where d is a p -dimensional function depending on an $(r \times 1)$ vector of fixed effects, β , and a $(k \times 1)$ vector of random effects b_i associated with individual i . Equation 3.2 describes how β_i vary among individuals, due to explained systematics correlation with individual characteristics in a_i and to "unexplained" variation in the population of individuals, represented by b_i . Usually it is assumed that the distribution

of b_i is independent of a_i , with $E(b_i|a_i) = E(b_i) = 0$ and $\text{var}(b_i|a_i) = \text{var}(b_i) = D$. Parameter D is an unstructured covariance matrix that is the same for all i . D represents the magnitude of "unexplained" variation in the elements β_i and associations among them. A standard such assumption is $b_i \sim \mathcal{N}(0, D)$, where D is the magnitude of the random effect.

3.1.3 Model Contextualization

In the previous section, we present a theoretical overview of NLME models. In this sub-section, the model will be contextualized within the framework of the problem. As explained before, the model's objective is to predict the stress, $\sigma(\lambda)$, in a uniaxial tension test. Therefore, the model's response is the stress, and 'time' is the stretch. As explained in the previous subsection, we will not considered any possible relevant additional conditions. Thus, the following equation is obtained:

$$\sigma_{ij} = f(\lambda_{ij}, \beta_i) + e_{ij}, \quad j = 1, \dots, n_i. \quad (3.3)$$

The observations, resulted from the uniaxial tensile tests applied to vaginal tissues, follow a typical behavior. Illustrated in Figure 3.2.

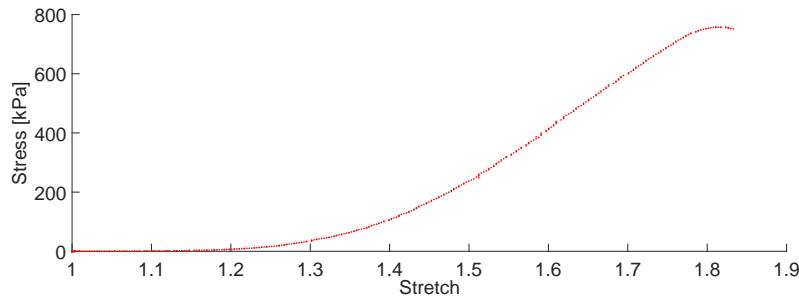


Figure 3.2: Stress(σ)-stretch(λ) curve of a patient's sample.

From figure 3.2, we can see that the graph is truncated just after stress, $\sigma(\lambda)$, reaches the ultimate tensile stress. This is made due to two reasons. After the ultimate tensile stress, the increment of necking makes the measure of stress more complicated and subject to errors. In the daily life actions, it is rare that the vaginal tissue reaches its maximum stress. Therefore, data truncation allows error reduction and without implying the loss of critical information.

As related before, choose the structure of $f(\lambda_{ij}, \beta_i)$ is one of the most important factors of the model's success. To reproduce the behavior of $\sigma(\lambda)$ accurately, we tested several equations in the fittings. It is worth mentioning that the physical meaning of the individual parameters, $\beta_i = (\beta_{1i}, \beta_{2i}, \dots, \beta_{pi}) = (c_{1i}, c_{2i}, c_{pi})$, depends on the equation structure. Where the vector c_{ji} contains the constants to be fitted for each individual. For this concrete case of study, the proposed equations are as follows:

1. Gauss equation

$$f(.) = c_{1i} \cdot e^{-\left(\frac{\lambda_i - c_{2i}}{c_{3i}}\right)^2} \quad (3.4)$$

2. Gompertz

$$f(.) = c_{1i} \cdot e^{-c_{2i} \cdot e^{-c_{3i} \cdot \lambda_i}} \quad (3.5)$$

3. Logistic

$$f(.) = \frac{c_{1i}}{1 + e^{-c_{2i} \cdot (\lambda_i - c_{3i})}} \quad (3.6)$$

In a first approach, these equations were chosen based on their ability to represent the uniaxial tensile test with the lowest number of variables possible. The usage of many variables introduces over-fitting problems, that can compromise the model. We considered that the Gauss equations, Gompertz and Logistic have the right balance between relying on a few variables and include a large part of the system dynamics.

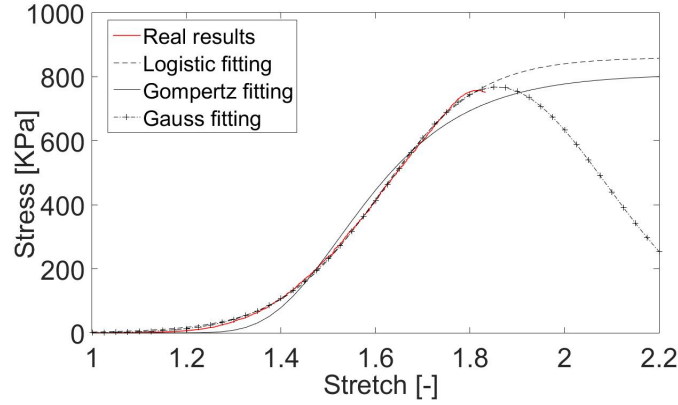


Figure 3.3: Fittings using the three proposed equations applied to a Patient sample.

As can be seen from figure 3.3, the three equations provide suitable approximations until the point that data is truncated. After the ultimate tensile stress, the behavior of the three fittings diverge. Gompertz and logistic equations follow a horizontal asymptote, thus failing to represent the typical response of vaginal tissue. In opposition, Gauss curve steadily decreases its value after the point of maximum stress, thereby ensuring a better approximation to the reality.

Non-linear mixed effects models rely on the level of correlation between the individual features and the response that is supposed to predict. This study will use the following patients' co-variables:

- Age;
- Years of menopause;
- Duration of hormonal therapy;
- Number of pregnancies;
- Number of natural childbirths.

These co-variables were chosen based on their availability in the database and theories proposed in the literature that indicates an influence on mechanical properties of vaginal tissue and preliminary results that show their correlation with the stress curve.

In this problem context, theoretically inferring the vector β_i is hard to achieve. Hence the process of defining β_i vector is fundamentally empirical. After the definition of $f(.)$ function, its parameters should be related to the co-variables of each patient. As assumed before, $\beta_i = (c_{1i}, c_{2i}, c_{3i}) = d(a_i, \beta, b_i)$, where

d , in this case, is a 3-dimensional function since $f(\cdot)$ has three parameters. We should be aware that the definition of d directly depends on the $f(\cdot)$ function chosen before.

We started by investigating the relation between the patient features and the parameters of the $f(\cdot)$ function. This study proposes four different approaches to the dependencies mentioned before.

1. Polynomial combination of co-variables with a defined maximum degree,

Order 1:

$$d_p = w_0 + w_1 a_1 + w_2 a_2 + w_3 a_1 a_2 + b_p, \quad w = (w_0, \dots, w_3) = \text{constant}, \quad (3.7)$$

Order 2:

$$d_p = w_0 + w_1 a_1 + w_2 a_2 + w_3 a_1 a_2 + w_4 a_1^2 + w_5 a_1^2 a_2 + w_6 a_2^2 + w_7 a_1 a_2^2 + w_8 a_1^2 a_2^2 + b_p, \quad w = (w_0, \dots, w_8) = \text{constant} \quad (3.8)$$

The three equations mentioned above, are examples of possible polynomial structures of vector d_p with two co-variables and a specific maximum degree. The equation, that describes the variation of the number of terms in a polynomial equation, is given by:

$$Nr.terms = 2 + p \sum_{l=0}^{nvar-1} (p+1)^l + b_p, \quad p \in IN_0, \quad nvar \in IN, \quad (3.9)$$

where $nvar$ and p refer to the number of co-variables and maximum degree chosen. As can be seen in equation (3.9), the number of constants to be fitted greatly increases as the degree gets higher. The same problem also arises when the number of co-variables used is increased.

Knowing that the number of variables is one of our primary concerns, this study proposes a randomly selection of a limited number of terms that will be used in vector d structure. This procedure aims to reduce the equation degrees of freedom. Hence, this proposal allows the size truncation of the equations that will compose the vector d . Several compositions, with different numbers of terms, are experimented to calculate and determine the best approximation.

2. Sum of exponential terms can be expressed by:

$$d_p = w_0 + \sum_{l=1}^{nvar} w_{lp} \cdot e^{-k_{lp} \cdot a_l} + b_p \quad (3.10)$$

Where k is a vector constituted by the constants to be fitted. The number of constants is written as the function of the co-variables number:

$$Nr.terms = 2 + 2.nvar \quad (3.11)$$

3. Fourier equation, which can be written as:

$$d_p = w_0 + \sum_{l=1}^{nvar} (w_{lp} \cdot \sin(w_{lp} \cdot a_l) + k_{lp} \cdot \cos(w_{lp} \cdot a_l)) + b_p \quad (3.12)$$

This equation assumes an oscillatory behavior of v_p parameters. Where the number of terms is defined by:

$$Nr.terms = 2 + 3 \cdot nvar \quad (3.13)$$

4. Assuming that the co-variables do not have any influence,

$$d_p = w_p + b_p. \quad (3.14)$$

The purpose of this approach is to verify if the co-variables are introducing meaningful information in the model and if they are, determine how much they are improving the predictions. The number of terms is defined by:

$$Nr.terms = 2 \quad (3.15)$$

The vector of fixed parameters, β , is given by the concatenation of all vectors of constants involved in the p -dimensional vector d .

As demonstrated in this section, the success of model predictions depends on a large variety of factors. In this type of models, the choices of f and d are the most critical decisions. Due to the lack of knowledge about which variables have influence and the impossibility of theoretical deduce the equations that govern the mechanical behavior of human tissues, we are only able to calculate local solutions inside the spectrum of structure types tested. Therefore, the process of defining $f(\cdot)$ and $d(\cdot)$ functions can be considered a heuristic algorithm.

3.2 Outliers detection in time series

Having in mind that this study is working with real data, it is essential to introduce the outliers subject. Hence, this section will explain the relevance of this topic on the overall study, beginning with the presentation of the outliers definition.

An outlier is defined as an observation that discrepant compared with the remaining data. In other words, is an element that does not fit the general pattern of the data [40].

The subject addressed is a particular case of outliers universe because it is only related to time series. They can be expressed as a set of data points indexed in time order, where the observations can be or not equally spaced in time. As explained in the previous sections, the graphs of the uniaxial tensile tests are not in order of time, but of stretch. So it is necessary to interpret the stretch as time.

As described before, in experimental studies there is always the possibility of having data subject to errors. From the previously enumerated sources, the failures originated in the tests measurements failures are worth to be mention again.

However, having outliers in the data set does not necessarily mean that occurred an error in gathering the data. There may have been an unknown reason that only affected one set of samples thus interfering with the test results. In this situation, the set of samples will be considered outliers because their results are skewed and do not follow the general pattern. Also there are real biological outliers, that exhibit a behavior that is not expected given the corresponding covariates.

The processes of identifying outliers are a topic of growing interest for several reasons. Being uncorrelated with the remaining observations, they can have a significant influence on the overall results, leading the analysis to incorrect conclusions. Therefore it is utmost importance to previously identify and remove them to develop better analyses, models and achieve useful conclusion.

In the literature, several methods were developed to detect and exclude outliers. To accomplish it, Battaglia et al [41] developed a method that allows the evaluation of the data points based on their fittings, where the approximations are made resorting to autoregressive models. If the model is proved to be suitable for the time series, it is considered an outlier observations that present a great discrepancy. It is important to have in mind that this approach can be applied to a large variety of problems. In modeling financial markets, these methods are applied to prevent model parameters estimation biases, incorrect conclusions and poor volatility forecasts. These markets are commonly modeled using autoregressive conditional heteroscedastic models. Using Monte Carlo experiments in this kind of models, several authors concluded that remove outliers from the dataset improve the accuracy of the prediction interval compared to those in which they are ignored [42].

Several publications have appeared in recent years documenting methods to overcome the presence of outliers in time series. These methods, in spite of identifying outliers, adopt robust estimation procedures to avoid their influence. According to Sarnaglia in [43], the time series are modeled resorting to periodic autoregressive moving average models. To estimate the model parameters, they proposed a new algorithm, where robust estimators based on auto-covariance functions are used. This kind of approach allows the minimization of the influence of defective observations.

Typically, outliers result from different kind of errors, however, in certain cases, they may represent a phenomena of interest [44]. In the literature, several studies that exemplify it. For example, according to Hauskrecht in [45], outliers detection based on previous data, can be used for improving healthcare practices. In this case, they represent unusual patient-management decisions, that may have occurred due to repetitive procedure errors. When an outlier is detected, an alert is sent to warn about the possibility of a bad medical decision.

Note that graphs from uniaxial tensile tests are two-dimensional. In this section, only outliers of univariate time series are going to be addressed. As previously reported, in our study context, the stretch has the same meaning as time.

When we refer outlier, we are referring to an entire sample or to single observations. The outliers related to isolated observations can be grouped into two categories: Additive and innovation outliers. The first group is related to an unexplained value in a single observation that it does not has correlation with others in the same sample. The second group is associated with perturbations which affect successive observations [41]. In figure 3.4, it is described the groups of outliers previously referred.

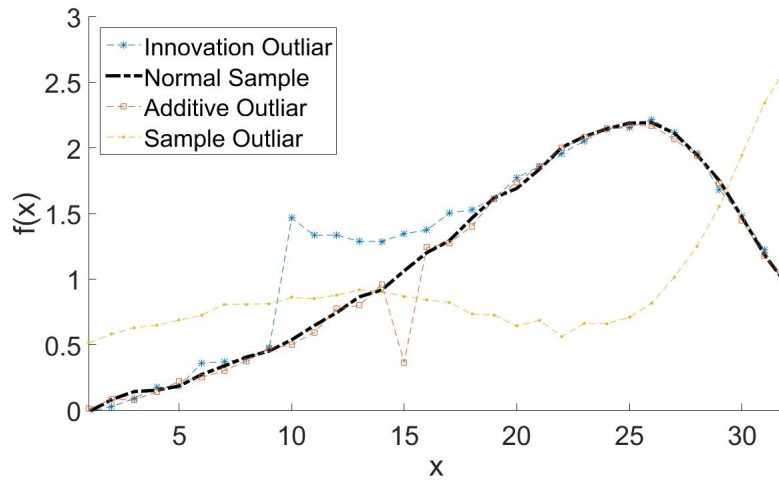


Figure 3.4: Example of the three outlier types proposed.

Even though all types of outliers can appear in the dataset, this study is going to focus on the sample outliers. In the tests, each curve contains a large quantity of points. Therefore outliers restricted to a short period of the curve have a small influence on the curve fitting. In the event of sample outlier, knowing that all the curve is affected, the curve fitting is completely skewed. Hence it is plausible only not to ignore sample outliers.

This work is focused on humans tissues and they are known for having a wide variety in their behavior both inter-individual and intra-individual. Therefore we can have samples from the same person that respond to and a mechanical test in very different ways. Many reasons may support this behavior. For example if one tissue is locally damaged, its mechanical properties will be affected. Hence when we test the same tissue in different spots, there is the possibility that the results of one test will be skewed by the damaged. Considerate that each person and each tissue is exposed to an enormous variety of environmental stimuli. We can try to measure the most relevant variables, but in fact, it is impossible to know all the inputs that influence each human tissue. When we put the problem in a wider perspective such as inter-individual samples, more factors will have an impact on the response of the same tissue type, such as lifestyle and genetics. Neither we can fully measure. Therefore, in a dataset the existence of outliers translate the difficulties in predict the mechanical behavior of that point due to the existence of distorted variables.

Regarding the models to be used, NLME model assigns the same weight to all the patient samples. Therefore, if one of them is very discrepant, the patient fitting accuracy is going to be affected. As consequence, the patients' attributes will lead to wrong $f(\cdot)$ parameters. When the number of samples per patients is relatively small, one outlier can have a significant influence in that particular patient fitting. If this problem occurs in several patients, the model accuracy is going to be severely affected. Since this study is going to work on a dataset with few patients and few samples per patient. A significant part of this study is will be dedicated to cleaning the dataset by removing discrepant observations

In this thesis, a new approach to identify and remove outliers from a dataset is also proposed, in order to improve the parameter estimation results. In order to understand the introduction of this method, we

have to realize that a NLME model includes the random effect component, b_i and that can be interpreted as the unexplained error that a sample has compared to the estimated general pattern. Assuming that, after the model is developed, the outliers have more probability of having greater error than the rest of data, we can deduce that the samples with a higher b have the highest chances of being outliers. The innovative part of this approach consists in relate random effects with outliers. Hence, this process is fundamentally empirical because we need to create the model to analyze the random effects of each data point. Therefore, this approach does not guarantee that the solution obtained corresponds to the optimal solution.

Concerning the number of outliers, when a dataset only has one outlier, its influence in the model is going to be small. However, when the number of outliers increases, their influence is going to be stronger in the parameters estimation. After a certain outliers percentage, they can disturb so much the $f(.)$ variables that they will start to be considered as valid data points. Therefore, removing the data points with greater error, in a straightforward way is a mistake because it can lead to misclassification problems. In a view to overcome this issue, we propose an approach based on experimenting several solutions, then classify as an outlier the data points that most deteriorate the model accuracy. The central proposal concept is that if we repeat the process of identifying and removing the "worst" data point and then create the next model resorting to the remaining data, the elements more times classified as an outlier have more probability of being one.

The definition of an outlier is not totally quantifiable, therefore with this proposed approach, there is no guarantee that the data point that we are identifying as an outlier is correct. So it is imperative the analysis of the data points that were removed and determine if there is a valid reason for the removal. It also be taken into account that before applying this process to the dataset, an evaluation must be performed to have a notion of how many outliers the method should identify.

3.3 Levenberg-Marquardt algorithm

Fit data to a particular nonlinear equation is one of the most relevant processes of this thesis. We perform this process resorting to MATLAB commands that apply specific algorithms, such as Levenberg-Marquardt and Trust-Region. In the present study both were tested. We chose Levenberg-Marquardt because it had fewer convergence problems which can cause the crash of the program implemented.

The algorithm chosen falls within the ambit of least-squares problem. This study dedicates the current section to describing this algorithm.

Levenberg-Marquardt (LM) method is one of the most popular gradient-based inversion solution methods for parameter estimation. Since it is a gradient-based method, it has the advantages of having high accuracy and efficiency. In gradient-based methods, the evaluation of sensitivity coefficients is the critical issue. However, they are difficult to be calculated precisely if multi-dimensions, transient states and nonlinearities are involved. Therefore, if the problem dimension is too big, this method becomes computationally intensive [46].

This algorithm can be considered as a combination of gradient descent technique and Gauss-Newton

method, in which, a damping factor λ is added to the diagonal entries of the Gauss-Newton Hessian matrix. The damping factor, assuming only positive values, help stabilize the Hessian matrix and it is essential to improve the algorithm convergence. [47]

Least squares problems arise when approximating a parametrized function to a set of measured data points by minimizing the sum of the squares of the errors between data points and the function. Nonlinear least squares problems occur when the function is not linear in the parameters. Solving this problem involves minimizing the following function:

$$\min f(X) = \|F(X)\|_2^2 = \min \sum_i^m F_i^2(X) \quad (3.16)$$

Where $F(X)$ is a vector defined by:

$$F(X) = \begin{bmatrix} \bar{\varphi}(X, t_1) - \bar{y}(t_1) \\ \bar{\varphi}(X, t_2) - \bar{y}(t_2) \\ \dots \\ \bar{\varphi}(X, t_m) - \bar{y}(t_m) \end{bmatrix}$$

Where $\bar{y}(t_m)$ is the measured data at time m and $\bar{\varphi}(X, t_m)$, dependent on time and a vector of n parameters X to a set of m data points, represents the data given by the fitting function. In other words, $F(X)$ is the difference between the prediction, $\bar{\varphi}(X, t_m)$, and the measured points, $\bar{y}(t_m)$. Note that $\bar{y}(t_m)$ and $\bar{\varphi}(X, t_m)$ are already divided by y_m .

The minimization of $f(X)$ must be carrier out iteratively because the function $\bar{\varphi}(X, t_m)$ is nonlinear. Therefore the value found in each iteration is used to find a the step, to be added to parameters X , that reduces $f(X)$. This step can be divided into two components, the first given by gradient descent technique and the second by Gauss-Newton method.

The steepest descent method makes a general minimization updating parameters in the direction opposite to the gradient of the objective function.

The gradient of $f(X)$ concerning the parameters is given by:

$$\frac{\partial}{\partial X} f(X) = 2 \cdot (\bar{\varphi}(X, t) - \bar{y}(t))^\top \cdot J \quad (3.17)$$

Where the Jacobian matrix $[\partial \bar{y} / \partial \bar{X}]$ describes the sensibility of \bar{y} to the variation in the parameters X . The parameter update referred above is given by:

$$h_{dg} = \alpha \cdot J^\top \cdot (\bar{\varphi}(X, t) - \bar{y}(t)) \quad (3.18)$$

The positive scalar α represents the length of the step in the steepest-descent direction.

The other part of the step update is related to the Gauss-Newton method. As mention before, this approach minimizes the sum of squares of the objective function. For problems with a moderate size, the Gauss-Newton method typically converges much faster than gradient-descent methods. The step update given by this method is summarized by the following equation:

$$[J^T J]h_{gn} = J^T(\bar{\varphi}(X, t) - \bar{y}(t)) \quad (3.19)$$

The Levenberg-Marquardt algorithm uses a search direction that is a solution of the following linear set of equations:

$$(JJ^T + \lambda \text{diag}(J^T J))d_{lm} = J^T(\bar{\varphi}(X, t) - \bar{y}(t)). \quad (3.20)$$

Where the scalar λ controls both magnitude and direction of step d_{lm} . When λ is zero, the direction d_{lm} is identical to the Gauss-Newton step. On the contrary, if it tends to infinity, d tends towards the steepest descent direction, with magnitude going to zero. The λ is initialized to be large so that the first updates steps use mostly the descendant direction. When the objective function approaches a local minimum, the value of λ decrease, the Gauss-Newton gradually gains preponderance and the solution accelerates to the local minimum.

Chapter 4

Implementation

In this chapter, the process of creating the Nonlinear Mixed-effect model based on the uniaxial tensile test data will be explained.

The process of achieving the optimal model implies experiment several solutions until the best results are obtained. Hence, the development of a program, fully automatic, that allows the creation of models with different characteristics is proposed. Such as $f(\cdot)$ and $d(\cdot)$ structures, individual co-variables and other options explained in the next sub-sections.

The program is implemented in the MATLAB platform. We chose this platform because there are available several commands that facilitate the process of developing the models. MATLAB is also one of the most powerful computational tools to solve engineering problems.

As mentioned in previous sections, the purpose of this work is not only to develop a model to a specific database but should also allow the adaptation to different databases. In future work, testing several databases will allow a deeper understanding of how the individual characteristics influence the models' results and reduce the possibility of conclusions being skewed by data acquisition errors.

Besides solving the required problems, the user-friendliness was also a factor to take in account. In other words, should be easy to the user introducing required options and check the models' accuracy. This can be accomplished by presenting to the user graphs and meaningful statistics, that show the real extent of the difference between model predictions and the actual uniaxial tensile test data obtained.

4.1 Program generic flowchart

In this sub-section, the generic program flowchart is presented. The program is divided into several modules to make easier the understanding of how it works. Each modulus represents the flow of information.

The actions that lead to the creation of the model can be summarized in Figure 4.1. As can be seen, the program can be split into four major parts. Each part represents a MATLAB block that was created to make specific tasks. Each block is composed of one or more MATLAB functions that are responsible for smaller assignments.

MATLAB program starts by treating the data, which includes truncating the test data points, minimizing the noise and transforming the graph force/elongation in stress/stretch. Afterwards, in blocks two and three, $f(\cdot)$ and $d(\cdot)$ structures are computed using iterative methods. The final action is related to the creation of the model, using the information previously obtained and presenting the results.

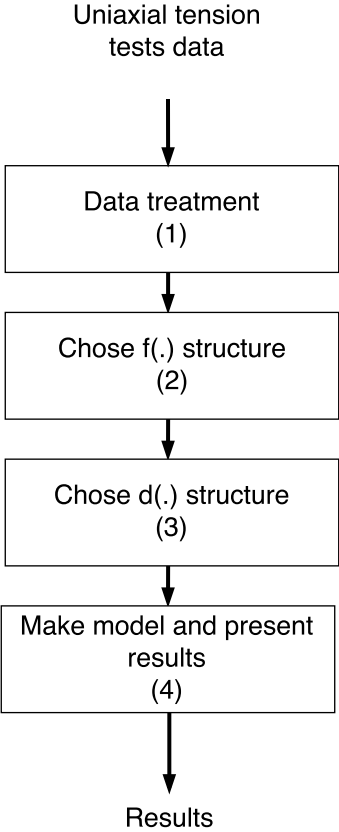


Figure 4.1: Simplified model of program flowchart.

It is worth mentioning that all relevant information is stored in an excel file, allowing a later analysis of the processes that occurred in the program.

4.1.1 Data processing

Data processing is a fundamental phase in the model development. This block transforms and structures the data to the model can easily interpret them.

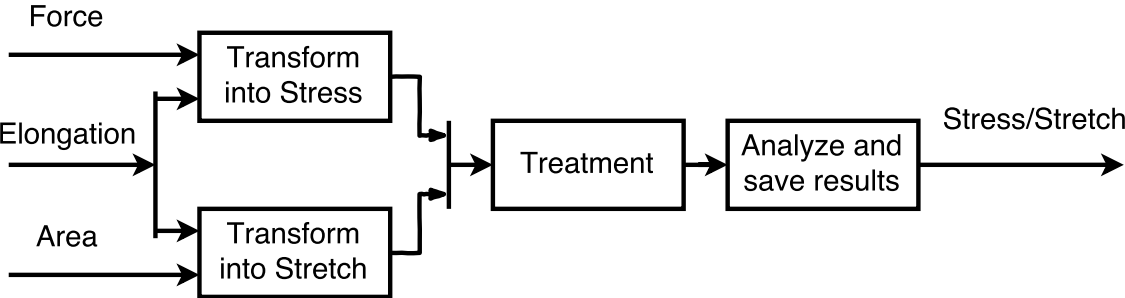


Figure 4.2: Detailed view of data treatment block.

From Figure 4.2, it can be seen that this block is divided in four main operations.

As explained in the last chapter, the force and elongation obtained from the uniaxial tensile test have to be transformed in engineering variables, stress (σ) and stretch (λ). Force and elongation are imported from a text file and the sample geometric characteristics from an excel file.

Afterwards, stress/stretch curve has to be treated. Due to measurement errors, stress can reach negative values, which is physically impossible and therefore, in that case, stress is assumed to be zero. Since the most relevant curve part is located before the point of maximum stress, data is truncated after that value is reached. Since in this tests, a preload was applied, stress is not zero at the initial point. To equal zero, the stress measured at the beginning point in all curve points was subtracted

The last stage of this block is dedicated to analyze the stress/stretch and check if there are curves that show clear signals of errors. This pre-analysis is fundamental to approve the choice of outliers that the program will make, in the following block. All results are saved to future analysis.

4.1.2 Fitting observations

This block's main goal is to choose the more suitable $f(.)$ structure. Having the stress/stretch data points, we need to find which equation better fits the data.

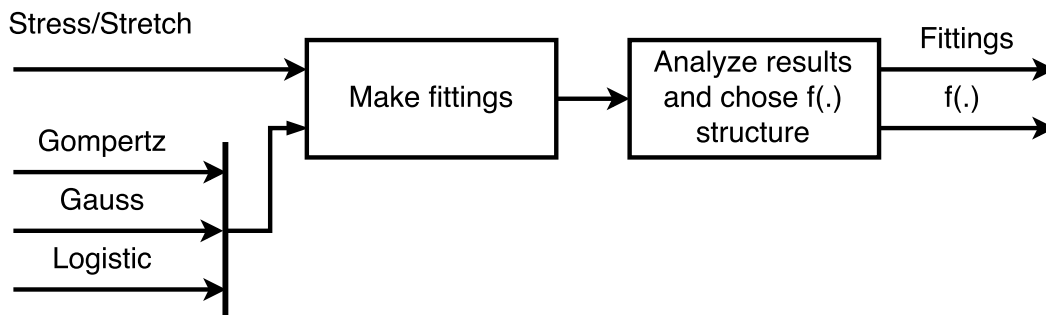


Figure 4.3: Detailed view of $f(.)$ fitting block.

As illustrated in Figure 4.3, the choice will be between three options: Gauss, Gompertz and Logistic. Their equations were described in the previous chapter: equation 3.4, 3.5, 3.6, respectively.

The fitting is made resorting to the MATLAB command *fit*. This command adjusts the parameters of a given model to the data to minimize an objective function. We choose to apply the Levenberg-Marquardt algorithm to solve the nonlinear least-squares problem. To use this command, we need to introduce stress/stretch data and the equation structure. The model parameters and some meaningful statistics, such as adjusted R-square and the root mean squared error (RMSE) are then returned.

RMSE represents the sample standard deviation of the differences between predicted values and observed values. It is defined by the root of the mean of the sums of the square of the error between the observation and the prediction. R-square is a value that indicates the proportion of the variance in the dependent variable that can be predictable from the independent variables. In cases when it assumes the value one, only the independent variables affect the observed values. Adjusted R-square is a modified version of R-square. This parameter only increases its value when the new term improves the model

more than would be expected by chance. The information obtained with these statistics is very relevant because it shows the fitting quality.

In our case, the program fits each patient sample individually and grouped by patients. In case of patients fittings, the correspondent data samples are concatenated and then inserted in the "fit" command. The resulting parameters are the ones that better describe the behavior of all the samples combined.

The following step is related to the analysis of the results and to the choice of the structure that better describes the data. After that each sample and patient parameters are passed to next program block. It should be mentioned that all the graphs of experimental data and the calculated equations are saved, in order to allow their visualization after the program closes.

4.1.3 Fitting covariables

The $d(.)$ fitting block main purpose is find the relation between patient co-variables and the parameters of the $f(.)$ equation. In order to be more rigorous, we should have used the fittings of each patient, but instead, we use the fittings of each sample. Since the database is small, we need more points to make the parameters adjustment of the $d(.)$ equations vector. The fittings of each patient are performed only for visual analysis purposes.

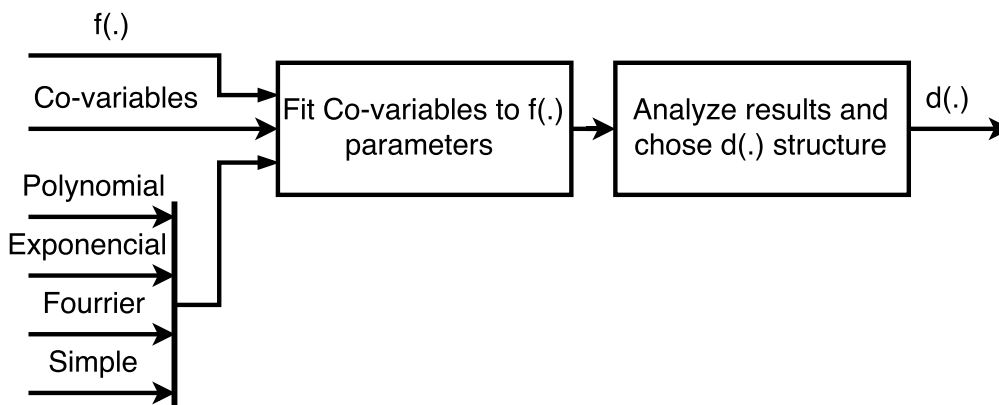


Figure 4.4: Detailed view of $d(.)$ fitting block.

The block present in Figure 4.4 has as inputs the chosen $f(.)$ structure, their respective sample parameters, the patients co-variables and the possibilities of $d(.)$ equations available for selection.

As explained previously, we experimented several structures for the $d(.)$ equations. First, the process with the polynomial will be described. In this form, to calculate the parameters of the equations, we use the MATLAB command *fitlm*. The function creates a regression model with the structure chosen by the user. As referred in the last chapter, we do not know in advance what is the best combination of terms that better fits the data. Therefore, the program tests many combinations of terms and chooses the ones with the lowest root mean square error. The number of terms used should be as low as possible because more terms imply more parameters to be adjusted. The user should take into account that increasing the number of parameters should be followed with the increment of the data volume. After the operation of achieving the $d(.)$ is done, we use the MATLAB command *step* to remove terms that do not have a

significant correlation with the observations. This action is performed to simplify the equations and to eliminate variables that introduce noise into the model.

When the $d(\cdot)$ form is a sum of exponential terms or is a Fourier equation, the process is slightly different. In those cases, we use the MATLAB command *fit*, as we used in $f(\cdot)$ structure fitting where the co-variables and the equation form are the inputs. Then, the command returns the adjusted parameters and the fitting results. Depending on the database, sometimes this command fails in making the fitting. The main reasons are the lack of correlation between data and the large decision space. It is understood by decision space, the intervals in which the parameters can vary. This block runs the command several times, each time using different intervals and different starting points. Resorting to this results, we choose the one with the lowest RMSE.

Figure 4.4 presents the four types of equations as inputs of the program block but, in reality, the simple function is not apart of it. Since it does not depend on individual co-variables, it is shown just for better understanding purposes.

In the end, based on the results, we choose the best $d(\cdot)$ structure and save the results for a posterior analysis.

4.1.4 Create a Nonlinear mixed effects model

The last program stage is to develop a Nonlinear mixed effects model. This block includes several small operations that will be detailed in this subsection.

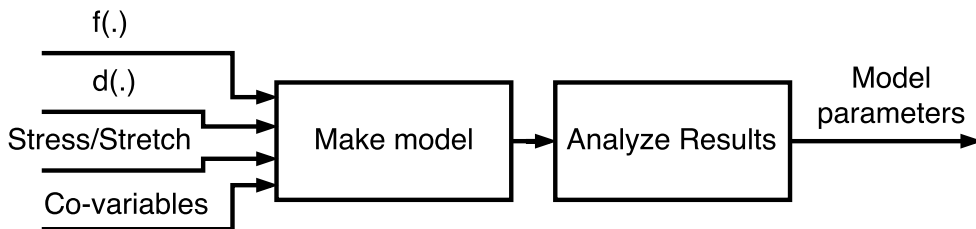


Figure 4.5: Detailed view of model creation block.

As can be seen in Figure 4.5, to implement the model we use the information gathered in the previous programs block such as: $f(\cdot)$, $d(\cdot)$, stress/stretch curves and individual co-variables. Inside the MATLAB block, we proceed to the organization of the stress/stretch data and creating the matrix A and the initial guess for the vector β . A and β_0 are defined, in order to satisfy the following equation:

$$\beta_i = A(a_i) \cdot \beta + b_i \quad (4.1)$$

As we assumed in the previous chapter, $f(\cdot)$ function depends on three parameters, we can write the last equation in a different notation:

$$\begin{bmatrix} \beta_{1i} \\ \beta_{2i} \\ \beta_{3i} \end{bmatrix} = \begin{bmatrix} [A_{1i}] & 0 & 0 \\ 0 & [A_{2i}] & 0 \\ 0 & 0 & [A_{3i}] \end{bmatrix} \cdot \begin{bmatrix} [\beta_1] \\ [\beta_2] \\ [\beta_3] \end{bmatrix} + \begin{bmatrix} b_{1i} \\ b_{2i} \\ b_{3i} \end{bmatrix}$$

Where $A_{1i}, A_{2i}, A_{3i}, \beta_1, \beta_2, \beta_3$ are vectors whose size depends on how many terms the structure d_i has for each $f(\cdot)$ parameter. If we multiply matrix A_i by vector β and sum b_i , we obtain the equation d_i given in the previous block. It should be noted that vector β cannot depend on co-variables in opposition to the matrix A .

The described model is developed resorting to the MATLAB command *nlmefit*, as presented in Figure 4.6

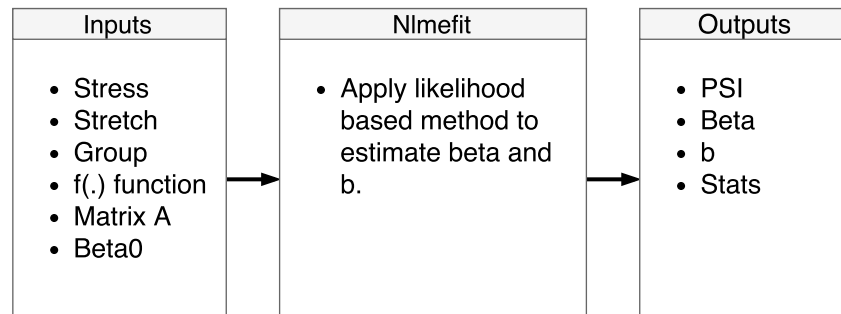


Figure 4.6: Information diagram of command *nlmefit*

There is a substantial number of inferential methods to implement a nonlinear mixed effects model. The method chosen to approximate the model likelihood is the First-order Laplacian approximation. For model simplification purposes, we will not consider that random effects are correlated with each other. The inputs and outputs of this MATLAB command can be seen in Figure 4.6. Regarding the outputs, PSI represents the estimated covariance matrix for the random effects. β_0 is the vector of the fixed effects. b_j accounts for the random effects correspondent for each observation. The last output is the "stats" which contains several indicators related to model creation process and the quality of its predictions. After the model creation, we analyze the results, investigating if they are coherent to the tests' data. If not, it is important to evaluate which parameters/tests are distorting the overall performance.

4.2 Iterative process to remove outliers

Having the generic program implemented, we performed a few preliminary tests and noticed that some of them seemed uncorrelated with the rest of the data. Consequently, those tests affected negatively the results of the model created. What led this thesis to address the outliers issue.

As defined before, an outlier can be described as an observation point that is inconsistent with the remaining data. In experimental data, outliers are frequent because the sources of error propagation can be minimized, but not completely eliminated.

In this study an innovative algorithm was implemented in order to identify and remove outliers from a dataset. Following the generic program philosophy previously explained, this algorithm is essentially a set of iterative cycles that determine the points that are repeatedly poorly explained by the models, as outliers. The developed method main goal is to improve the model accuracy.

The program operation sequence including the iterative process can be seen in Figure 4.7. This iterative process is carried out after $f(\cdot)$ and $d(\cdot)$ structures are chosen and the $f(\cdot)$ parameters of every sample are defined.

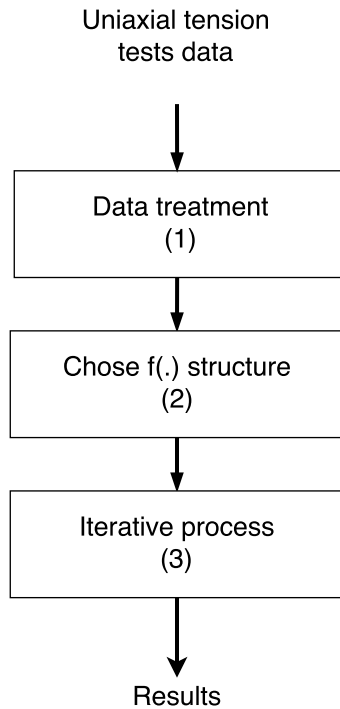


Figure 4.7: Iterative process flow chart

The Figure 4.8 presents the sequence of all the actions executed by the developed algorithm. This method is composed of three main cycles and fifteen actions. Each action represents a MATLAB function and each cycle represents a MATLAB *for* loop. First, the user should chooses the number in which each cycle stops and continues to the next action. In Figure 4.8 these numbers are expressed with the letters x , z and w . Each cycle has an action identified with the number one because it is the first action that runs inside of the cycle. It is worth mentioning that since $d(.)$ structure is defined, the parameters will be adjusted inside the iterative block. The development of the model and the $d(.)$ equation fittings follow the methods described in subsections 4.1.3 and 4.1.4.

In Figure 4.8, the first referred MATLAB function is related to the organization of stress/stretch data and their respective adjusted parameters. Once finished this step, a preliminary identification of outliers is performed. This action is carried out by executing the fitting of the co-variables with the adjusted parameters of $f(.)$ function. From the results, the outliers are those with higher cook distance coefficient. This coefficient measures the influence of a data point when a least-squares regression analysis is performed. The increment of the outliers distance from the rest of the data, will grant them a higher influence in the overall results. Therefore the applied method is valid to perform the initialization of the outliers vector. Note that, the initialization is only made in the polynomial structure of the vector $d(.)$, in the remaining cases it is not carried out due to the lack of information of the MATLAB command *fit*.

Following the initialization, the algorithm enters in its first loop. In the first iteration, $d(.)$ fitting is executed without z outliers identified in the initialization. The second loop takes advantage of the information retrieved from the MATLAB command *nlmefit*. When the model is created, we can access to the estimated random effects of each observation. Knowing that they represent the unexplained part of the response, we can assume that outliers will have a greater random effect. This assumption is the main premise

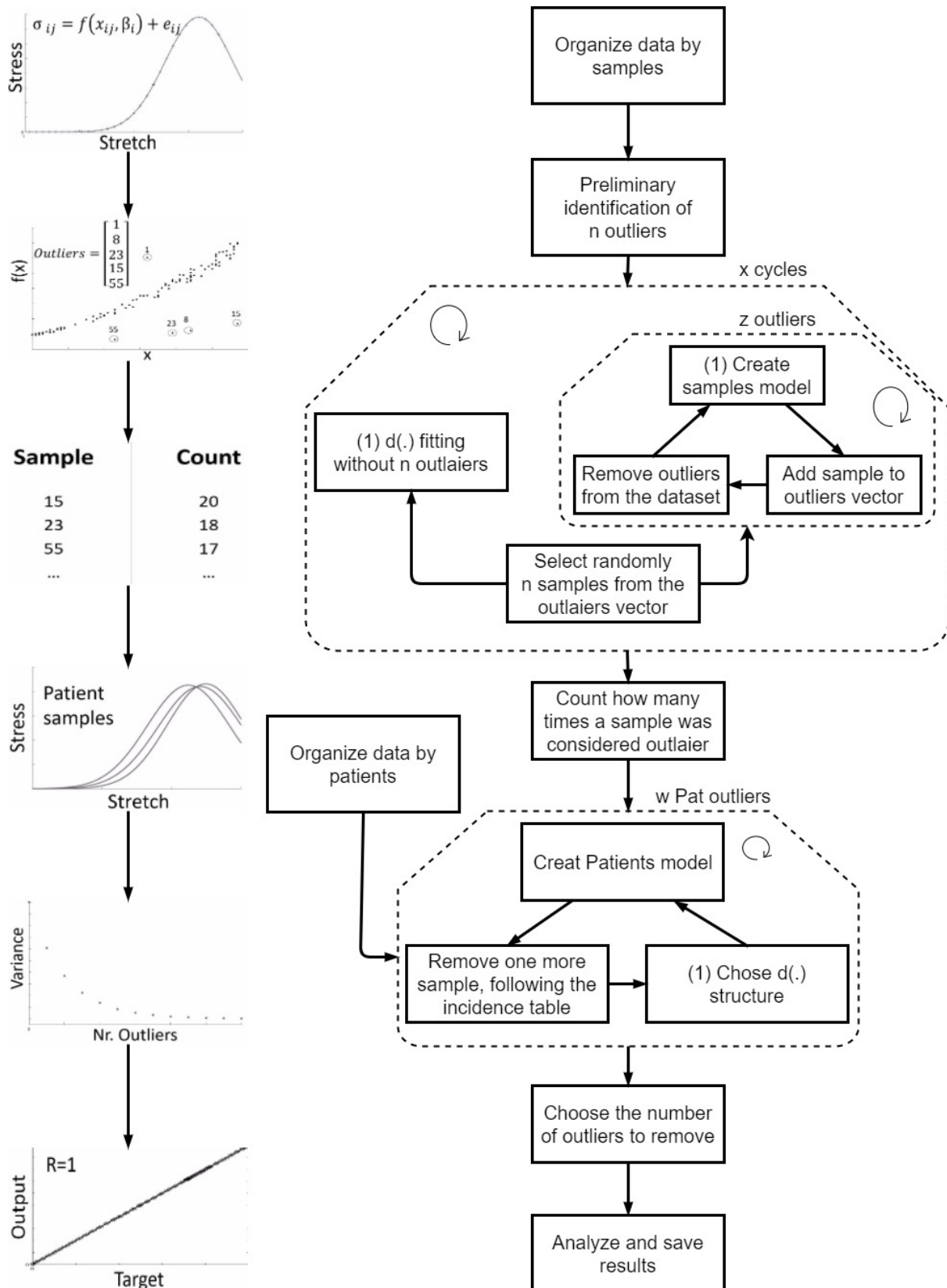


Figure 4.8: Flow chart of Iterative process implemented to identify and exclude outliers

of our iterative process. Hence, it is important to summarize the loop path: The first step is to create the model where it assumes that the observation that is less explained by the model is an outlier. Once

identified, the second step is to remove this outlier from the dataset. It should be noted that the second loop runs z times and starts with the complete database and an empty outliers vector. After z loops, z outliers were removed and added to the outliers vector. Back in the first loop, the vector n data points are randomly chosen from the outliers vector and then the $d(\cdot)$ fitting operation starts again. We decided to limit the number of outliers to n elements because when the model is created, if an observation does not participate in the $d(\cdot)$ fitting, the probability of having a greater random effect is higher. Therefore, if the number of cycles is large enough by choosing some data points randomly, the model will give a chance of every observation to participate in $d(\cdot)$ fitting. This process will improve the algorithm robustness.

The following function counts how many times a sample was considered an outlier and order the samples by the number of occurrences. We gathered the information into an incidence table. In this step, we resorted to MATLAB function responsible for organizing the data by patients to be used in the implement of the patients model. This action is performed by concatenating the stress/stretch vectors, which belong to the same patient. Then the algorithm enters in the third loop which runs w times. The loop starts by executing $d(\cdot)$ fittings using the data ordered by samples. Later, the patients model is created, resorting to the data organized by patients. Realize that only in this step, the model results are related to each patient and not to each sample. After this phase, the algorithm selects from incidence table the sample in position w and remove it from the dataset. Then, the fittings and patient model are obtained without the selected samples. This loop main purpose is to investigate the influence of the outliers removal, from the dataset, in the overall results. The fact that the model is based on equations that depend on the fitting add value to our iterative process.

In order to choose the optimal number of outliers to be excluded, the user can resort to several indicators that show the impact of the outliers removal. In the following phase, the program is responsible for creating the model with specifications decided by the user. Finally, the algorithm presents the final model results and several indicators that evaluate the its predictions quality.

A relevant aspect to take into account is the values of variables x , z and w are high enough. It is expected that when their values are increased, the process accuracy in identifying and excluding outliers will improve. An obvious disadvantage is the computational effort that will be necessary to enlarge the number of iterations. However is essential to balance the accuracy needed and computational effort available. Hence, in order to achieve better results, the number of models created is greatly raised. Consequently, the computational time follows the trend.

Chapter 5

Datasets description

As explained in the previous chapter, this study will implement NLME models resorting to several datasets. The data used to obtain the results allow this study to take a large variety of conclusions. We divided the current chapter into two sections, each one with different purposes. The first section reports to the real dataset of uniaxial tensile tests applied on vaginal tissue. The second section is related to the artificial data created to ensure that the implementation of the model works satisfactorily.

5.1 Artificial data

In order to test the process reliability, we generated several datasets which represents a challenge on its own, due to the complexity of the system.

The approach implemented is entirely original. Consequently, we need to validate the algorithm intensively to verify its robustness. The datasets created in this section have a similar structure to the real dataset to minimize the modifications on the program code and to be as realistic as possible.

To facilitate the process of creating datasets, we implemented an algorithm in the MATLAB platform. In order to maintain some degree of coherence among them, we establish several rules. Therefore, the results of different datasets can be compared without the risk of the conclusions being bias.

At this point, it is essential to describe the chosen parameters and how they vary among the different datasets:

1. Age, l_1 , assumes random values between a specific interval,

$$l_1 = \mathcal{U}(30, 9).$$

2. Menopause status, l_2 , is defined based on a normal distribution,

$$X_1 \sim \mathcal{N}(47.5, 5),$$

if $X_1 < \text{Age menopause}$, $l_2 = \text{true}$, else $l_2 = \text{false}$.

3. Age at the time of menopause, l_3 , depends on the value calculated previously,

$$\text{if } l_2 = \text{true}, l_3 = X_1.$$

4. Existence of hormonal therapy, l_4 , has a 32% chance of being true, if the woman is on menopause,

$$X_2 = \mathcal{U}(0, 1) ,$$

$$\text{if } l_2 = \text{true} \wedge X_2 < 0.3 , l_4 = \text{true} ,$$

$$\text{if } l_2 = \text{true} \wedge X_2 \geq 0.3 , l_4 = \text{false} .$$

5. Age when hormonal therapy started, l_5 , is equal to the age when the menopause started

$$\text{if } l_4 = \text{true}, l_5 = l_4.$$

6. Age when hormonal therapy ended, l_6 , is equal to the value l_5 plus a number generated randomly between 1 and 5,

$$X_3 = \mathcal{U}(1; 5),$$

$$\text{if } l_4 = \text{true} \wedge l_5 + X_3 \leq l_1, l_6 = l_5 + X_3 ,$$

$$\text{if } l_4 = \text{true} \wedge l_5 + X_3 > l_1, l_6 = l_1 .$$

7. Number of pregnancies, l_7 follows a normal distribution, which is based on the average number of pregnancies in Portugal during the last 90 years,

$$l_7 = \mathcal{N}(1 + l_1 \cdot 2.8/100, 1).$$

8. Number of natural childbirths, l_8 . We achieve an equation that defines the probability of having a pregnancy ended in abortion, then we applied it to the number of pregnancies calculated previously,

$$P_{abortion} = \sum_{i=1}^k ((1 - (1.8 \times 10^{-3} \cdot l_1 - 2.6 \times 10^{-2})) \cdot (1 - (-5.7 \times 10^{-3} \cdot l_1 + 0.5))) ,$$

$$l_8 = l_7 - \sum_{i=1}^{l_7} (\mathcal{U}(0, 1) \geq P_{abortion}) .$$

We assumed that all children born by natural childbirth to simplify the dataset creation.

Following the presented equations, we assumed that the age, l_1 , is the most important parameter because the remaining variables are dependent of its value.

Intended to have a better understanding of the equations responsible for the simulated co-variables, we have generated a dataset containing 150000 data points.

These data points are described in 5.1. As can be seen, age is uniformly distributed in the age interval between 30 to 90 years old. The probability of women being on menopause increase with age, following a normal distribution curve. The number of pregnancies and resulting children depends on the age. This dependency occurs because the number of pregnancies and the abortion rate have been steadily decreasing over the years in Portugal. Therefore, the oldest a woman is, the larger is her probability of having more pregnancies. The same applies to the number of abortions. Figure 5.1 shows the mean number of pregnancies and children by age. As can be seen, both parameters have greater values in older women.

As explained in a previous chapter, we decided to transform the initial parameters, to improve the models' accuracy.

The transformed parameters are shown in the following list:

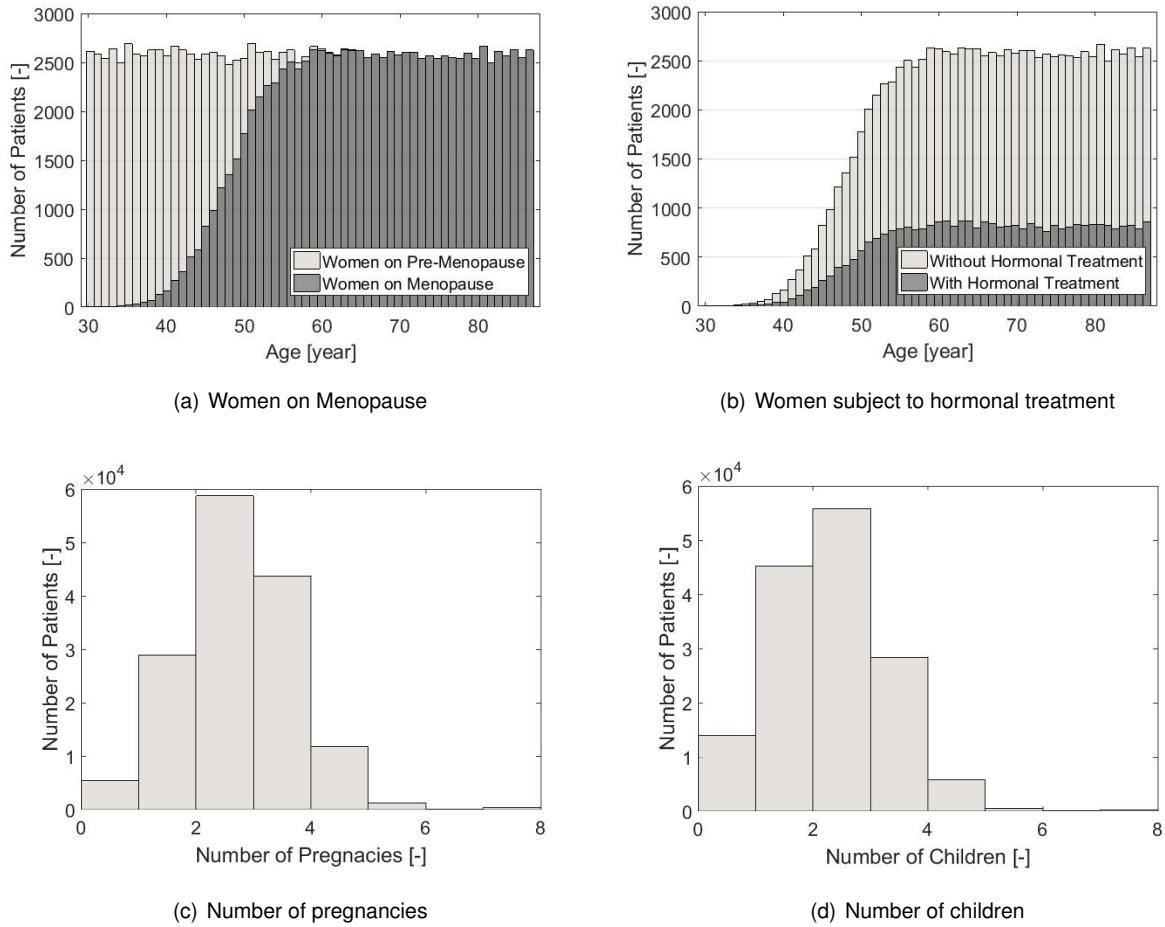


Figure 5.1: Co-variables generated in an example dataset

- Age, $A = l_1$;
- Years of menopause, $YM = l_3 - l_1$;
- Duration of hormonal therapy, $DHT = l_6 - l_5$;
- Number of pregnancies, $NP = l_7$;
- Number of natural childbirths, $NVB = l_8$.

These transformations prevent the model of working with variables that can only assume two values, such the menopause status, l_2 and the existence of hormonal therapy, l_4 .

Assuming that the real case can be modeled using NLME models, the next step in the artificial is to create the equations that relate the individual attributes with curve points.

As explained previously, the equations were developed, to the generated dataset be an approximation from the real. It should be remembered that the best equation that describes the uniaxial tensile test curve is the Gauss equation, which can be expressed by the following curve:

$$y = c_1 \cdot e^{-\left(\frac{x-c_2}{c_3}\right)^2} \quad (5.1)$$

Gauss equation depends on three parameters. Therefore we need to develop three different equations. This thesis selected the polynomial structure for the d equation vector and the fittings were made resorting to the *fitlm* command.

To choose the parameters values in the polynomial equation, we analyze the intervals which the real data varied. Then the values were assigned to the variables based on that information. The equations vector is represented in NLME models by the variable $\beta_i = d(a_i, \beta, b_i)$. Assuming that $\bar{\beta}_i$ accounts for the developed equations vector, it can be presented in the following form:

$$\bar{\beta}_i = \begin{bmatrix} 0.45W_1^2 - 1.4W_1 + 80 \\ -0.1W_5^2 + 0.8W_5 + 0.05W_2 + 4.7 \\ 0.004W_1 + 0.15W_5 + 0.6 \end{bmatrix}$$

Since in real systems all the measurements have associated errors to simulate real data as close as possible, noise was added. In this case, the noise is proportional to the equation value. This study stipulated that, in modulus, it can vary between zero and a certain percentage of remaining equation value. These can be presented in the following equation :

$$\bar{\beta}_i = \begin{bmatrix} 0.45W_1^2 - 1.4W_1 + 80 \\ -0.1W_5^2 + 0.8W_5 + 0.05W_2 + 4.7 \\ 0.004W_1 + 0.15W_5 + 0.6 \end{bmatrix} \cdot (1 + \alpha_i)$$

Where α is the variable that determines the error amplitude. Noise is one of the variables that we will vary, in order to test how our algorithm handles errors, for example in the test measurements.

The algorithm that this study presents is intended to develop the models overcoming the possibility of having tests that are not correlated with the remaining data. These tests are assuming to be outliers. In a previous chapter, it was explained the method that this algorithm uses to identify and remove outliers from a data set to develop the models more accurately. In this section, the ability to detect and remove outliers will be tested.

In the dataset, a certain percentage of outliers, P_{Out} , is going to be introduced. Several tests, containing different numbers of outliers, will be made, in order to check if the algorithm can identify and remove them. If they are not eliminated in the filtering process, it should be registered their influence in the modeling process. Besides their number, another important factor is how much the points curve will be "dislocated" in the outliers case. This deviation is going to be represented by the variable dv . So if a point is an outlier, its parameters will be purposely adulterated following the next rule:

$$\bar{\beta}_i = \begin{bmatrix} 0.45W_1^2 - 1.4W_1 + 80 \\ -0.1W_5^2 + 0.8W_5 + 0.05W_2 + 4.7 \\ 0.004W_1 + 0.15W_5 + 0.6 \end{bmatrix} \cdot (1 \pm dv_i)$$

Variable dv_i in modulus is equal for the three equation, but it is randomly decided if it is positive or negative for each one.

In a fitting process, the influence of a point increases according to its distance to remaining points.

Therefore d value will determine the outliers preponderance in the dataset. Vary these two variables, d and α , will attest the algorithm's resilience to the presence of outliers in the dataset.

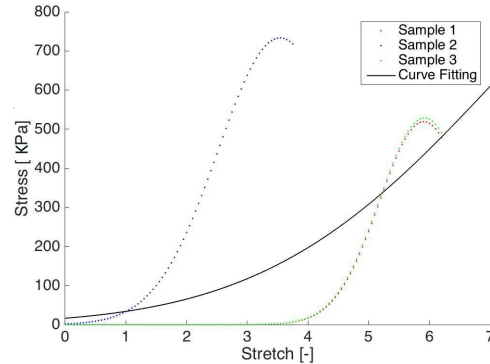


Figure 5.2: Three generated samples of one patient

In Figure 5.2, it is represented three tests. One of them is an outlier. As can be seen, the variation applied in the $f(\cdot)$ parameters affected the entire curve, make it stand out from the remaining samples of the same patient. It is also represented, the fitting using the three samples. As consequence of the presence of the outlier, the fitting quality is very poorly. It fails to represent the samples that are correlated with patient's co-variables. This situation can affect the estimation of $\bar{\beta}_i$. Consequently the overall results. We can also note that, because of the added noise, the normal samples are not equal. This discrepancy is proportional to the amplitude of the error introduced, α .

Fifty patients containing three or four samples compose the datasets. In each dataset, we change its parameters to fulfill the objectives proposed. In average each dataset has 175 samples. The variables that will differentiate each test are the error, the percentage of outliers and the the deviation of the outliers' parameters. We decide to limit the number of outliers to 20% of the dataset length because after that the algorithm takes to much time to generate the models and usually real datasets have a lower value of discrepant observations.

5.2 Real data analysis

This section is dedicated to describing the real data gathered. We will present some mean full statistics that help the understanding of the influence of the data in the results obtained. The information required to implement a NLME model includes the observations of the uniaxial tensile tests and the co-variables of every patient.

In this phase, we need to transform the force and elongation into stress and stretch. Therefore, since we also have the information regarding the geometrical properties of the samples during the tests, the algorithm has now the necessary conditions to execute this transformation automatically.

The co-variables gathered and the transformation made to improve the models accuracy is summarized in Figure 5.3. The notation adopted for the co-variables considered is the following:

- Age = Age ;

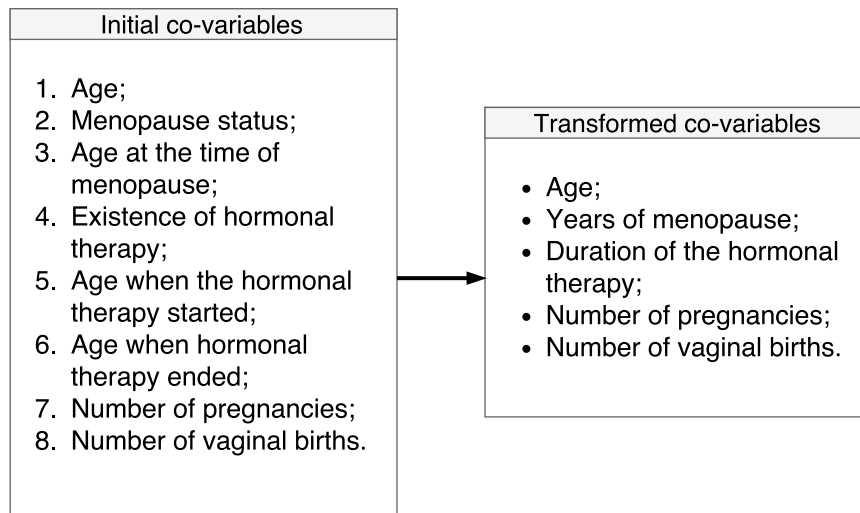


Figure 5.3: Variables transformation

- Years of menopause = YM ;
- Duration of hormonal therapy = DHT ;
- Number of pregnancies = NP ;
- Number of vaginal births = NVB .

At this point, it is important to understand the several reasons why the transformations were performed. It is easier for the model to manipulate continuous variables. The number of variables is reduced allowing a faster convergence and decreases the possibility of over-fitting. Over-fitting is a relevant problem because, as will be explained later, the dataset is not very large. Finally, we also assumed that the birth by cesarean does not influence the mechanical properties of vaginal tissue.

In this section, we will present the statistics regarding the already transformed variables because they are the inputs for the model. Consequently, it is easier to relate them with the results.

In Table 5.1, the real dataset that this thesis will use is described. Although, we have information regarding 29 patients, we only selected the patients with complete information because we intended to avoid missing data problems. In the same table, the number of valid samples there are for each patient is also explicit. Note that, every patient has at least one valid representation. For a better precision of the mechanical properties of the tissue, have several samples per patient is essential, since having more tests improves the robustness to the presence of outliers. Back to the previous table, there is one patient that matches the limit condition, when he has only one valid sample.

Table 5.2 summarizes the statistics regarding the co-variables. For each one, the parameters arithmetic mean, standard deviation, minimum and maximum are presented.

In Table A.1, the most relevant properties of each valid sample are described, such as maximum stress, stretch when the maximum stress is reached, thickness, length and width. In total, this study resorts to 89 valid samples.

For each variable shown in Table A.1, the Table 5.3 presents some meaningful statistics, such as arithmetic mean, standard deviation, minimum and maximum. As can be seen, in average the sample's

Table 5.1: Patients and their co-variables present in the dataset.

Patient ID	Age [Year]	YM [Year]	DHT [Year]	NP [-]	NVB [-]	Number of Samples [-]
Pat-17	79	34	0	1	1	6
Pat-18	64	14	0	3	3	3
Pat-19	72	22	0	4	4	6
Pat-20	49	3	0	5	3	6
Pat-23	74	26	0	2	2	4
Pat-24	59	2	0	5	5	6
Pat-25	78	33	0	6	6	4
Pat-26	84	32	0	4	4	6
Pat-27	67	13	1	6	2	2
Pat-28	38	0	0	4	4	2
Pat-29	66	11	5	2	2	2
Pat-30	68	26	0	2	2	4
Pat-31	57	7	0	4	2	6
Pat-32	60	13	5	4	4	2
Pat-33	68	25	0	4	4	2
Pat-38	56	6	6	4	3	4
Pat-49	66	12	5	3	3	2
Pat-50	44	0	0	4	4	1
Pat-51	83	43	0	10	9	2
Pat-52	65	17	1	0	0	2
Pat-53	69	19	0	0	0	2
Pat-54	45	0	0	2	2	3
Pat-55	57	6	0,5	3	3	3
Pat-57	56	6	0	2	2	3
Pat-60	75	30	0	3	3	3
Pat-62	68	19	0	3	3	4
Pat-66	49	0	0	2	2	2

Table 5.2: Statistical description of the patient co-variables.

	Age [Year]	YM [Year]	DHT [Year]	NP [-]	NVB [-]
Mean	63,6	15,5	0,9	3,4	3,0
SD	11,7	12,1	1,9	2,0	1,8
Min	38,0	0,0	0,0	0,0	0,0
Max	84,0	43,0	6,0	10,0	9,0

Table 5.3: Statistical description of the samples fittings

	Max Stress [KPa]	Stretch at max Stress [-]	Thickness [mm]	Length [mm]	width [mm]
Mean	545,9	1,9	1,5	10,4	8,3
SD	308,3	0,3	0,5	3,7	2,6
Min	139,4	1,5	0,7	4,6	3,0
Max	1565,9	2,7	3,2	23,2	17,5

maximum stress is 545.9 KPa, the minimum is 139.4 KPa and the maximum is 1565.9 KPa. Hence, we can conclude that there is a great discrepancy in the stress results across the samples. This disparity is lower in relation to the stretch in which the maximum stress is registered.

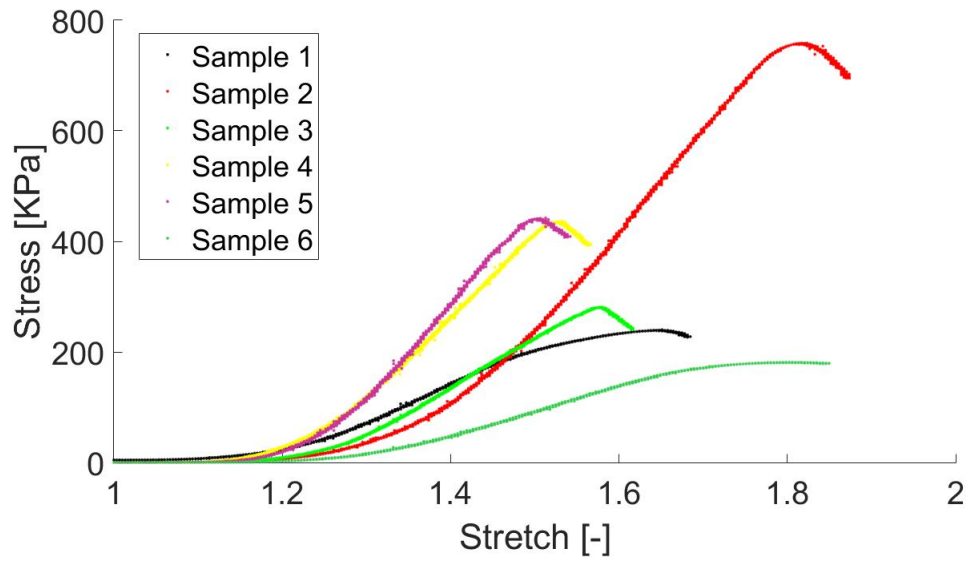


Figure 5.4: Tests on samples from the same patient

Finally, an example of the uniaxial tensile test applied to several samples of the same patient is presented. Figure 5.4 shows the results of uniaxial tensile tests applied on six samples from the Patient 17. This example confirms a high variability of the trials' results intra-individual. In a first approach, a weak correlation among the samples was verified. Realize that in a perfect situation, all the curves should be very similar, indicating a close relationship between the patient characteristics and several tests.

Chapter 6

Model results

In this chapter, the results obtained by the procedure proposed on Chapter 4 applied to the data described in Chapter 5 will be presented. Based on the results obtained this study will be able to conclude in what degree the objectives proposed were achieved.

The tests were applied both on the artificial and real dataset. Each one has different goals. On the real, it is intended to evaluate if it is possible to model the mechanical behavior of vaginal tissues based on its co-variables. On the artificial, the objective is to estimate the performance of the developed algorithm. Several indicators will be presented to understand in which measure the models represents the dynamics behind the samples. The most relevant results shown are the computational effort, model accuracy, relevance of outliers and the robustness of the method proposed.

6.1 Artificial data

In this section, we will apply the algorithm proposed on the artificial datasets. In this section, we will apply the algorithm proposed on the artificial datasets. The influence of several variables on the models' overall results will be clarified, such as the percentage of outliers, the noise in the samples and the deviation of the outliers parameters. The algorithm will be tested to confirm if it accomplishes the objectives proposed.

This thesis proposes an iterative process with the datasets described in section 5.1. It was assumed that the $f(\cdot)$ function follows a Gauss curve and the $d(\cdot)$ is a polynomial equation vector. The co-variables used are de Age, YM and NVB. This approach is meant to approximate the tests with artificial data to the tests with the real data.

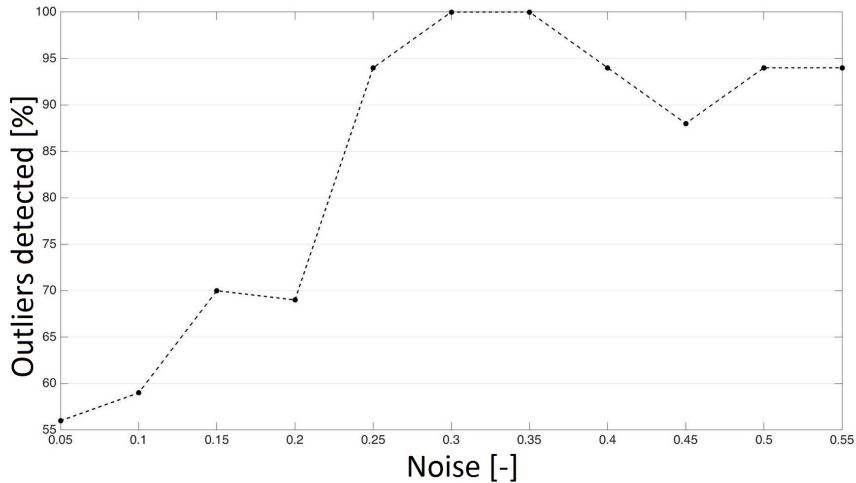
To uniform the experiments performed, we create several rules to the algorithm's parameters. Using the notation implemented in section 4.2, we present the following standards:

- Iterative cycles, $x = 0.4 \cdot NumberOutliers$;
- Length of the outliers vector, $z = 1.2 \cdot NumberOutliers$;
- Number of outliers removed per cycle, $n = 0.8 \cdot NumberOutliers$;

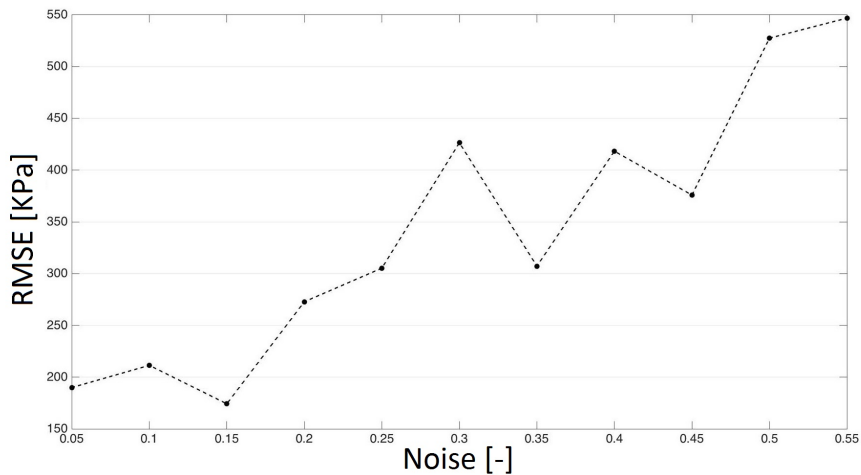
- Number of outliers removed from patient model, $w = 1.2 \cdot \text{NumberOutliers}$.

In average, the number of outliers present in the dataset is equal to 175 times their percentage.

First, we tested the influence the noise in the model accuracy and in iterative method capability to identify and remove outliers.



(a) Variation of the percentage of outliers detected with the noise, α



(b) Variation of the RMSE with the noise, α

Figure 6.1: Influence of noise added to the samples on the model results. Parameters $dv = 0.7$ and $P_{Out} = 10\%$.

As follows from Figure 6.1, the increase of noise impact the values of RMSE and the percentage of outliers detected. The error steadily increases as the noise become higher. This fact can be easily understood because noise will not allow that intra-individual samples being overlapped. Therefore, for each, there is always an error associated with the discrepancy of the samples. The previous Figure also shows that the algorithm increases its outliers detection accuracy until the noise is equal to 0.3 and then there is a slight decrease when the noise is greater than 0.35. All the outliers are identified when the noise value is between 0.3 and 0.35. So, we infer that introducing error helps the algorithm for the detection of outliers when the error introduced is smaller than the deviation of the outliers. This conclusion can be explained by several reasons. When there is no noise in the samples, the outliers

have a great preponderance in the fittings. They can affect so much the approximations that they become the valid samples, and the others are classified as outliers by the algorithm. When we add noise to the dataset, we are injecting variability in samples from the same individual. Therefore, the outliers are no longer as prominent as they were before and consequently lose some relevance in the fittings. In this situation, it is easier for the algorithm to detect and remove them. From this test, we conclude that the method stated by this thesis works better in situations where there is an intra-individual variability. This judgment can be very relevant in application to real datasets because they possess a high probability of having outliers and intra-individual samples containing deviations.

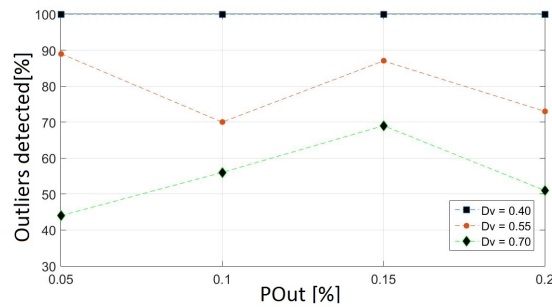


Figure 6.2: Three generated samples of one patient

In Figure 6.2 illustrates the influence of the deviation and the percentage of outliers on the rate of outliers detected. Three lines are presented, each one corresponds to a specific value of the deviation (0.4, 0.55, 0.7). A higher value of the deviation diminishes the algorithm identification ability. In the figure, smaller deviation always corresponds to lower accuracy. This conclusion can be explained by the relevance of the outliers on the fitting. When they are very dislocated from the remaining data, they tend to influence so much the function that they start to be considered the valid samples.

Also in Figure 6.2, it is shown the influence of the percentage of the outliers in the dataset on the rate of outliers identified. The three lines illustrated do not show a clear trend. They present variations, but not in a steady direction. Therefore, we can infer that there is no evident influence on the outcome presented.

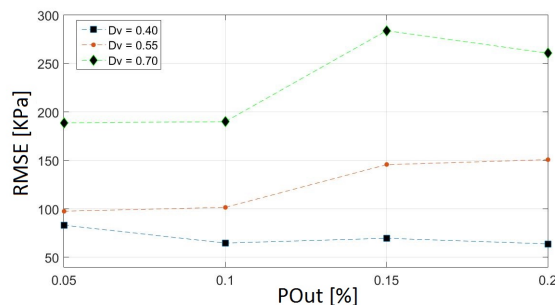


Figure 6.3: Three generated samples of one patient

This thesis evaluated the importance of the dataset parameters on the RMSE results. Figure 6.3 shows that for different deviations the outcomes are very distinct. The three lines presented correspond to three fixed deviations. When its value is more substantial, the RMSE becomes higher. This fact can be

explained by the conclusion given in the previous figure. If the algorithm has less precision in removing the outliers, the results will be less accurate naturally.

Additionally, from the Figure 6.3, we can perceive how the precision varies with the percentage of outliers added to the dataset. For deviation equal to 0.7 and 0.55, the error is more prominent when the number of outliers is increased. In the other line, there is no significant influence noticed. Combining the three patterns, we can not infer that the percentage of outliers, in the interval shown, affects the model RMSE. The variation presented is not sufficient to form a solid conclusion.

In summary, this section allowed a deeper understanding of how the algorithm behaves when it is exposed to diverse datasets. The most relevant conclusions are its ability to handle intra-individual variability across the dataset. Its efficiency to detect and remove outliers is improved. The outliers deviation is the most weakness of the algorithm because its accuracy is considerably affected when the outliers are very dislocated from the general pattern.

6.2 Real data

This section is dedicated to presentation of the results obtained by applying NLME models on uniaxial tensile tests data of vaginal tissue. In the first chapters, it was explained the reasons behind the application of this type of models, in patients' tissues. The primary objective is to predict mechanical properties of tissues based on patients individual characteristics. The indicators obtained during the modeling process shall quantify the degree of certainty of predictions given by the developed models. The choice of the MATLAB command, used to perform the fittings, was decided based on several factors, such as convergence speed, reliability, and accuracy.

One of their most significant weakness is the limit of the equations' dimension that the algorithm can handle. The command for polynomial equation can handle 3-dimensional equations whereas the others MATLAB's commands, for fitting, only handle 2-dimensional equations. Knowing that the algorithm applies an iterative cycle, it is essential that the command not have convergence problems. When it does not find a solution, it is vital that the command not crash because it is going to make the program stop. This problem is frequent in several commands tested. Taking every factor into account, we chose two MATLAB's commands, *fit* and *fitlm*. Command *fitlm* is the one that better satisfy the conditions imposed. So we will employ it preferentially.

As explained in the previous chapters, the equation used to describe the uniaxial tensile test observations is the Gauss equation.

Firstly, the algorithm assumes that each sample is independent. Only in the patient model estimation is assumed that samples from the same individual are correlated. So we executed fittings for both situations.

The fittings were performed resorting to the MATLAB command *fit*. Figures 6.4, 6.5 and 6.6 represent the relation between the estimated $f(\cdot)$ equation parameters and the co-variables. The five individual characteristics show the same behavior. Therefore, only present the variables that will use later in the models (Age, YM and NVB) are presented. The $f(\cdot)$ function's parameters display a very weak

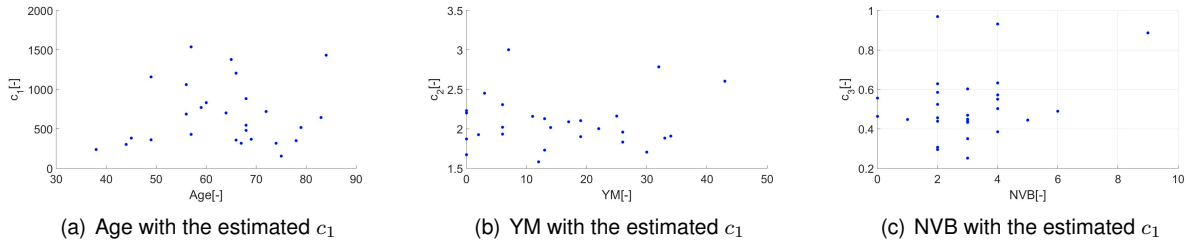


Figure 6.4: Relation between patients co-variables and estimated c_1

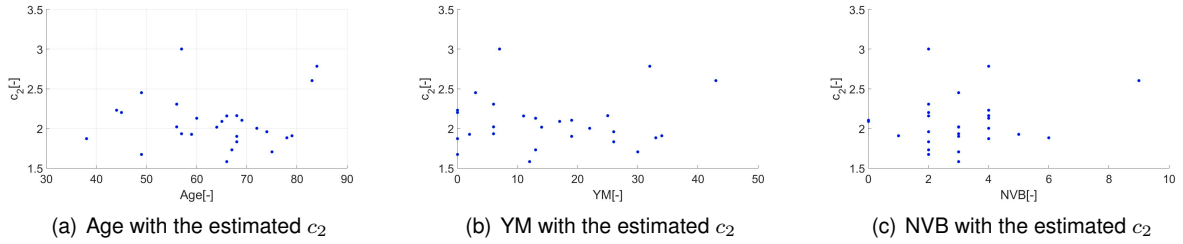


Figure 6.5: Relation between patients co-variables and estimated c_2

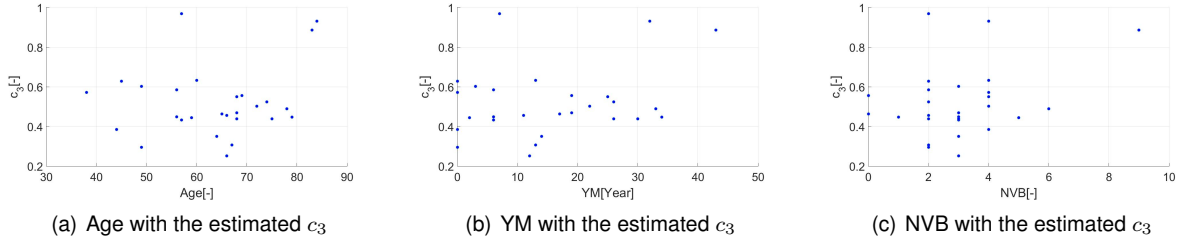


Figure 6.6: Relation between patients co-variables and estimated c_3

dependency with the co-variables. In a visual analysis, it is very complicated to find any trend in the data points. Therefore, we proceed to a mathematical analysis of the dependencies.

To have a deeper knowledge of how the patient's attributes influence the mechanical trials, we calculate the matrix Pearson correlation coefficient, also known as R. This coefficient quantifies the linear dependence between two variables. Its value varies between 1 and -1, where 1 or -1 means a total linear correlation and 0 indicates that there is no correlation.

Table 6.1: Correlation matrix between patients co-variables and fittings parameters

	Age [Year]	YM [Year]	DHT [Year]	NP [-]	NVB [-]
c_1	0,08	-0,02	0,23	0,01	-0,08
c_2	0,04	0,06	-0,16	0,27	0,19
c_3	0,18	0,26	-0,21	0,33	0,31

Table 6.1 presents the correlation coefficients calculated from the patients' fitting. As can be seen, the correlations are almost insignificant across all variables. This fact suggests that the co-variables have very few relevance in the experimental tests results.

Figures 6.4, 6.5, 6.6 and table 6.1 give a strong indication that is hard to obtain a model that represents the dataset satisfactorily. This problem can have the origin in the dataset, the fittings quality or in the

lack of ability to find the existing correlations.

Table 6.2: Statistical description of samples fittings.

	c_1 [-]	c_2 [-]	c_3 [-]
Mean	671,1	2,1	0,5
SD	387,0	0,3	0,2
Min	153,2	1,6	0,3
Max	1537,9	3,0	1,0

Table 6.2 summarizes the fittings results regarding the constants of the $f(\cdot)$ equation that are described in Table A.3 The statistics presented are very relevant to evaluate the model accuracy.

Table 6.3: Analysis of the fittings quality per sample

	RMSE [KPa]	R-Square [-]
Mean	7,23	1,00
SD	4,44	0,01
Min	1,57	0,88
Max	21,83	1,00

From Table 6.3, it can be seen the quality of the approximations performed regarding the uniaxial tensile tests. Two relevant indicators the RMSE and the R-square are presented. While the first measures the effective error between observations and the predicted value, the second quantifies the proportion of the variance in the output that is anticipated by the input. The average error is minimal, and the R-square is one in almost every sample. In the worst case, RMSE is equal to 21.83, and the coefficient of determination is equal to 0.88. Even in this situation, the fitting has a satisfactory quality. From the results, we can conclude that the Gauss equation makes an excellent approximation of the observations. It should be noted that we conclude the significance of the error by comparing it with the statistics presented in Table 6.2.

Table 6.4: Analysis of the fittings quality per patient

	RMSE [KPa]	R-Square [-]
Mean	78,03	0,83
SD	41,41	0,14
Min	4,57	0,49
Max	157,79	1,00

Table 6.4 presents the same indicators as the previous one. In this case, the information is concerning the patients fittings that are described in Table A.2. In other words, the samples are grouped by patients before we execute the estimations. The results presents show that the approximations are worst than in the previous situation. In average, the RMSE is nearly eleven times higher, and the R-square is about 27% smaller. The fittings are suitable when applied to a single test when we apply to several samples from the same patient the results get worst. Due to the high variability of the tests intra-individual, the

patients with a greater number of samples have poorest fittings quality.

The weak correlation intra-individual is illustrated in Figure 6.7. It is shown the uniaxial tensile tests of two patients. It is clear to conclude that for these examples will be difficult to prove any correlation between the $f(\cdot)$ equation parameters and the co-variables.

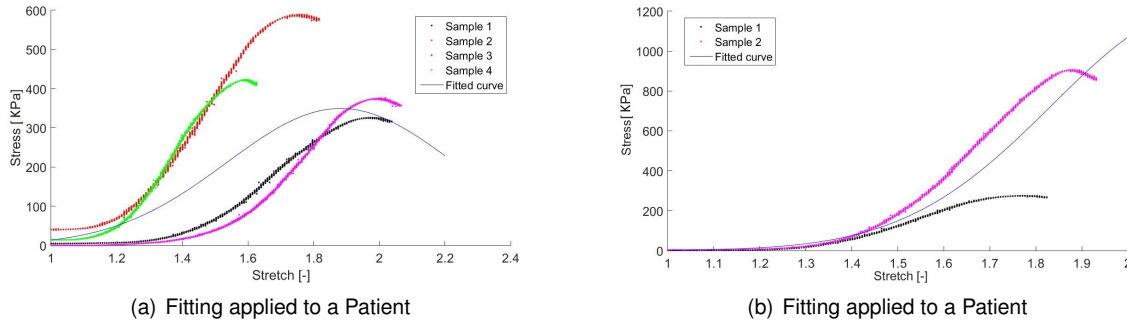


Figure 6.7: Example of two with a high inter-individual variability

Previously, it was explained that the MATLAB command *fitlm* is the one that better satisfies this study's requirements. Since we were not able to find an explicit dependency of the function, this study decided to assume a polynomial structure for the $d(\cdot)$ vector equation. The number of terms for each equation is between 2 and 3. Then, we apply the command *step* on the estimated equality to simplification purposes.

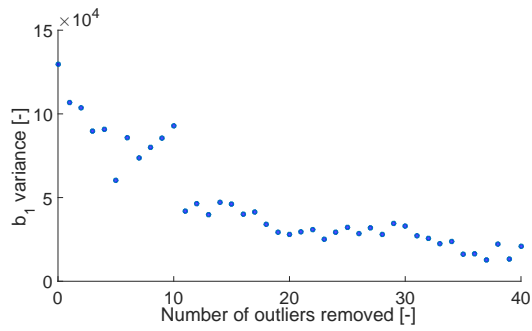
After several experiments, the co-variables that will be used are Age, YM and NVB. This is the combination that guarantee the best results.

After several tests performed, the parameters chosen for the algorithm are described in the following list:

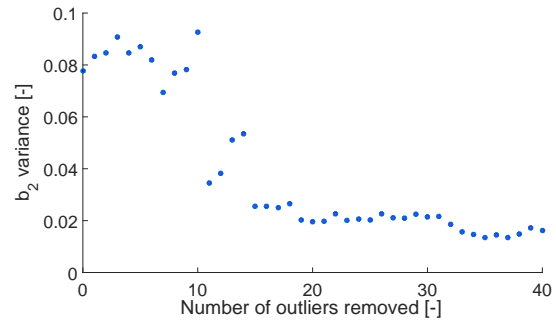
- Iterative cycles, $x = 20$;
- Length of the outliers vector, $z = 35$;
- Number of outliers removed per cycle, $n = 20$;
- Number of outliers removed from patient model, $w = 40$.

It should be noted that the choice made took in account several factors such as time spent, the percentage of possible outliers present in the data and possibility of remove all the samples from one patient. We decided that the algorithm must leave at least one test per patient, since we have a small dataset, we want to avoid removing individuals.

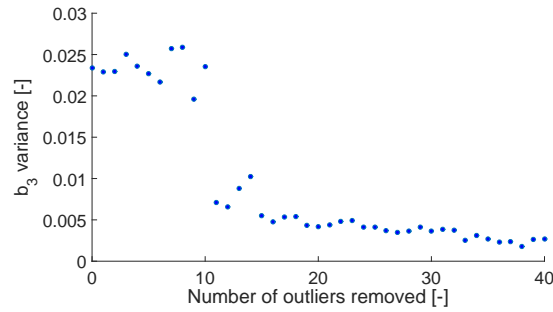
When the iterative process finishes, we have to decide how many outliers are to be removed. This decision is taken based on the variance of random effects. Figure 6.8 illustrates how they vary with the number of outliers removed. The samples to be removed are ordered by the number of times that were considered outliers by the algorithm. As can be seen, the variance of all random effects diminishes steadily as the algorithm is removing more samples. This behavior was expected because are being excluded the tests that are less explained by the model. Analyzing the graphs, we can see that the removal of the firsts 15 outliers had a significant impact on the variance but after that point, the variance



(a) β_1 variance with the number of outliers removed



(b) β_2 variance with the number of outliers removed



(c) β_3 variance with the number of outliers removed

Figure 6.8: Variation of the random effects variance with the number of outliers removed.

variation reaches a horizontal asymptote. In the three cases, the variation drops around 80% which means that removing erroneous tests allows the model to explain the remaining data better.

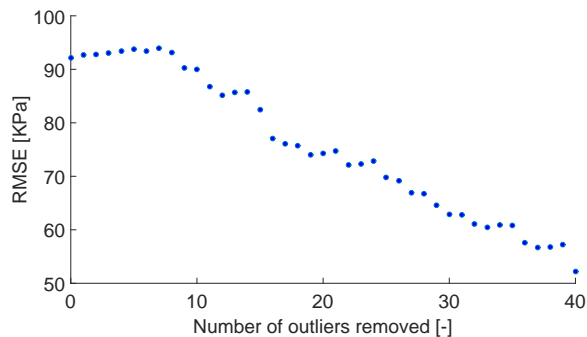


Figure 6.9: Variation of the model RMSE with the number of outliers removed.

The figure 6.9 illustrates the RMSE behavior when the algorithm removes the outliers. The error follows the predictable pattern. Starts equal to 91 and stays constant until ten samples are eliminated. After that point diminishes gradually. The error and the random effects variance follow different slopes because the model adds the effects. Therefore both parameters cannot be directly compared. The error firmly drops because the model has fewer samples to fit. Thus it can adjust more easily.

Combining the information given by the previous figures, we decide to eliminate 15 outliers. This decision took into account the balance between the lost of information and the model accuracy. If we proceeded to exclude more samples, the results would be better, but we were adjusting the dataset to the pretended results excessively.

From Table 6.5, the samples that were excluded from the dataset are presented. Patient 31 is the one

Table 6.5: Outliers identified

Outlier	Patient	Sample
1	Pat-20	4
2	Pat-26	6
3	Pat-28	2
4	Pat-31	1
5	Pat-31	2
6	Pat-31	5
7	Pat-31	6
8	Pat-32	2
9	Pat-38	1
10	Pat-38	2
11	Pat-38	4
12	Pat-49	1
13	Pat-52	2
14	Pat-54	1
15	Pat-54	2

that had more tests considered invalid. The tests applied to the samples from the referred patient are presented in Figure 6.10. The results show a substantial discrepancy of their mechanical behavior so it is reasonable that the algorithm considers several samples as outliers.

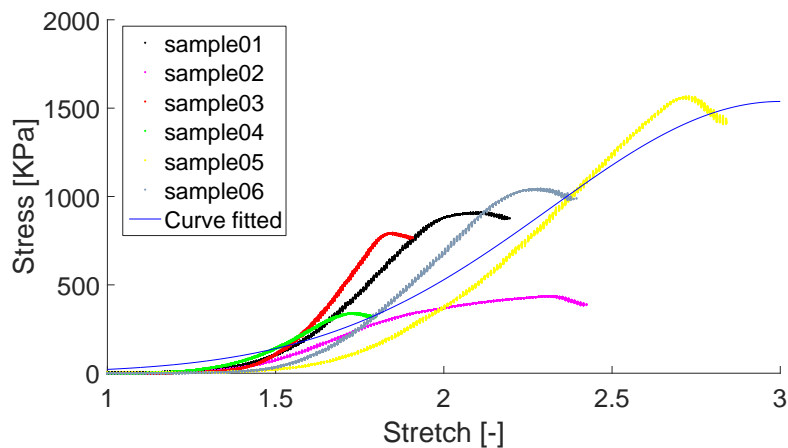


Figure 6.10: Samples of the Patient 31.

The algorithm chooses the outliers based on mathematical assumptions. We should always confirm if they are well selected. In Figure 6.11, we present an example of a sample that was considered an outlier. It can be seen that the excluded sample has a dynamic distinctly from the remaining tests. Its maximum stress is approximately the double of the other samples. This fact is a relevant indication that for some reason this test should not be valid. Therefore, this graph confirms that the iterative identifies the curves with a behavior that does not follow the general pattern.

As explained in previous chapters, a NLME model has a component of fixed effects and random effects. The fixed part is obtained by multiply the matrix A with the vector β . In an excellent situation, the result should be equal to constants of the function. In figure 6.12, it is presented the results given by the model and the real values. We consider that the real data is the one that was calculated in the fitting process.

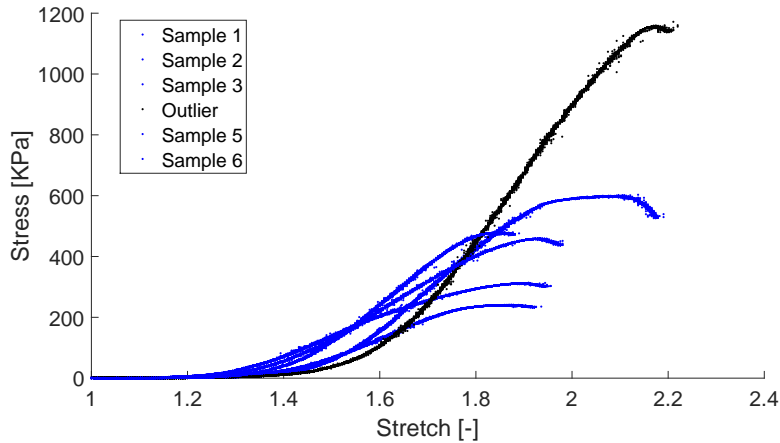
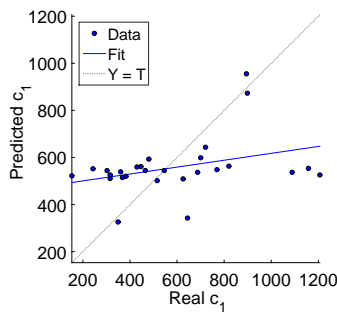
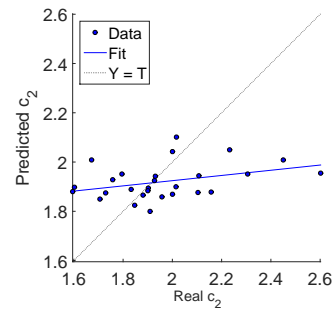


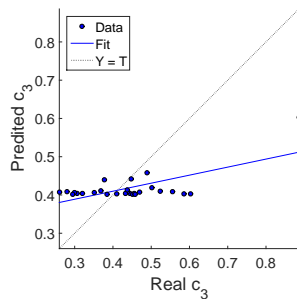
Figure 6.11: Example of an outliers removed by the algorithm.



(a) Comparison between c_1 given by the model and its real value.



(b) Comparison between c_2 given by the model and its real value.



(c) Comparison between c_3 given by the model and its real value.

Figure 6.12: Comparing the predicted values with the real values.

It can be seen that the model is not capable of providing a suitable relation between the co-variables the uniaxial tensile tests. The values predicted are not consistent with the calculated from the fittings. The figure also presents the tendency line. In the three situations, it is almost parallel with the horizontal axis. If the model was 100% accurate, the line should be making 45 degrees with the vertical axis and cross the zero.

Figure 6.13 presents the residuals diagram. We can conclude that exists a significant deviation in the parameters. Concerning c_1 , a relevant portion of the data has residuals above 20% of the constant arithmetic mean. In a first visual analysis, two points diverge from the remaining data, therefore they should have been considered outliers by the algorithm. Since the model does not fit them satisfactorily

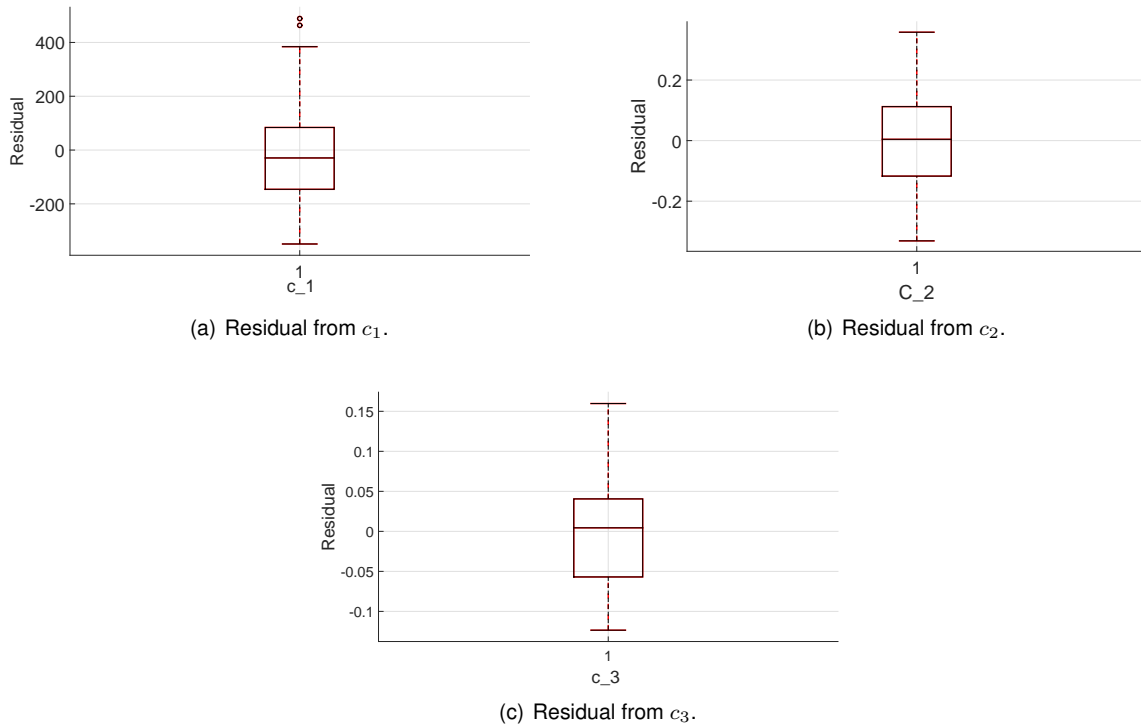


Figure 6.13: Residuals from the non-linear fit.

and they are part of a patient with more than 1 sample. In conclusion, the residual results are not satisfactory.

After analyzing the model results, we will describe the model obtained. The estimated covariance matrix is expressed by:

$$PSI = \begin{bmatrix} 4.4 \times 10^3 & 0 & 0 \\ 0 & 2.6 \times 10^{-2} & 0 \\ 0 & 0 & 5.2 \times 10^{-3} \end{bmatrix}$$

The variance of each random effect is very discrepant because of the scale of the parameter with each random effect is associated. The matrix agrees with the values expressed in Figure 6.8.

Table 6.6: Statistical analysis of the initial model and the final model

	Final model	First model	Variation [%]
RMSE [KPa]	82,20	91,90	-10,55
b_1 SD [-]	212,60	360,20	-40,98
b_2 SD [-]	0,16	0,28	-42,09
b_3 SD [-]	0,07	0,15	-52,63

In order to quantify the influence of the outliers removal, we compare the results of the first model containing all the samples and the final model without 15 outliers. The influence of the excluding process is expressed in Table 6.6. It is shown the error and the variance of the three random effects. All the indicators show that the final is better than the first one. The RMSE is reduced by 11%, which represents

a slight improvement. The variance of b_1 , b_2 and b_3 is reduced by 41%, 42% and 53% respectively. The variation in percentage is illustrates that the iterative process is a suitable tool to improve the NLME models. Excluding few samples, the model performance is increased. If we move the analysis, to the absolutes values of the final model, we conclude that the error is still large. The model was improved, but it cannot yet describe the system by the fixed effect part. Therefore the variance of the random effects is very high.

To evaluate the importance of the co-variables in the model implemented, we created a model that does not include them. When we compare the performance of both models, it is possible to infer if the individual's characteristics add relevant information to the model.

Table 6.7: Statistical analysis of the simple model and the final model

	Final model	Simple model	Variation [%]
RMSE [KPa]	82,20	97,52	-15,71
b_1 SD [-]	212,60	395,50	-46,25
b_2 SD [-]	0,16	0,32	-49,69
b_3 SD [-]	0,07	0,18	-60,00

Table 6.7 summarizes the error and variance of each model. As can be seen the all indicators are better the final model. The RMSE is reduced by 16%, which represents an improvement. The variance of b_1 , b_2 and b_3 is reduced by 46%, 50% and 60% respectively. Which means that the co-variables have a beneficial influence on the results. We should have in mind that the simple model utilize fewer parameters to describe the dataset and this results in less over-fitting problems. When we work with a small dataset, this issue is substantially increased. In this perspective, it has a slight advantage compared to the final that resorts to much more complicated equations and try to fit several variables recurring to just 72 samples. Therefore, with a more significant dataset, probably the difference between the two models would be substantial.

A primary objective of this thesis is to relate the co-variables with the equation of Gauss. The model adjusted the variable beta to obtain the best polynomial function that describes this relationship. Next, we present the resulting equations:

$$\begin{bmatrix} c_1 \\ c_2 \\ c_3 \end{bmatrix} = \begin{bmatrix} 419.6 - 1.1 \times 10^{-6} \cdot Age^2 \cdot YM^3 \cdot NVB + 3.9 \times 10^{-4} \cdot Age^3 \cdot NVB + 1.0 \times 10^{-10} \cdot Age^3 \cdot YM^3 \cdot NVB^3 + b_1 \\ 2.3 - 5.3 \times 10^{-3} \cdot Age + b_2 \\ 0.4 + 3.6 \times 10^{-8} \cdot YM^4 \cdot NVB - 8.7 \times 10^{-9} \cdot YM^4 \cdot NVB^3 + 2.9 \times 10^{-12} \cdot Age^3 \cdot YM^2 \cdot NVB^4 + b_3 \end{bmatrix}$$

The dependencies have different levels of complexity. We can note that the parameter c_2 is the simplest one. It only requires the age to be described. The other parameters need more terms and require more co-variables to be explained by an equation. From the equations, we can see that age effects all parameters. Menopause and number of vaginal births influence c_1 and c_2 . It should be noted that we limited the size of the polynomial functions. Without counting with the random effects, their maximum size is four.

After estimate the equations that relate the co-variables with the uniaxial tensile tests, it is essential to represent their behavior using example cases. From Figure 6.14, we can see the influence of age in the

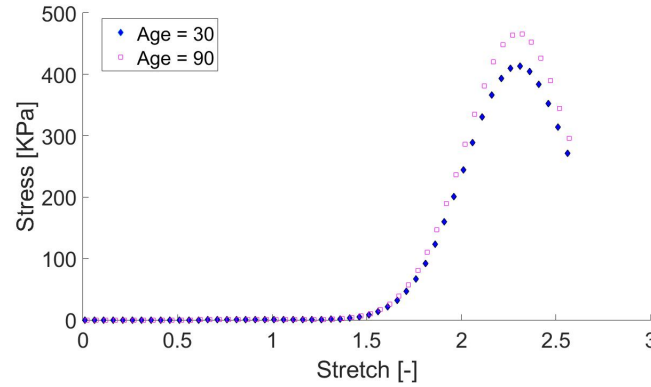


Figure 6.14: Influence of the Age on the predicted uniaxial tensile tests. Both samples have $NVB = 3$ and $YM = 15.5$.

equation obtained. There are expressed two predictions in the graph. The blue dotted line corresponds to a 30 years old and the other to a woman 90 years old. The oldest example has the highest maximum stress. This parameter is directly related with the c_1 that goes from 414 to 466, meaning a variation around 12%. The remaining parameters almost do not change.

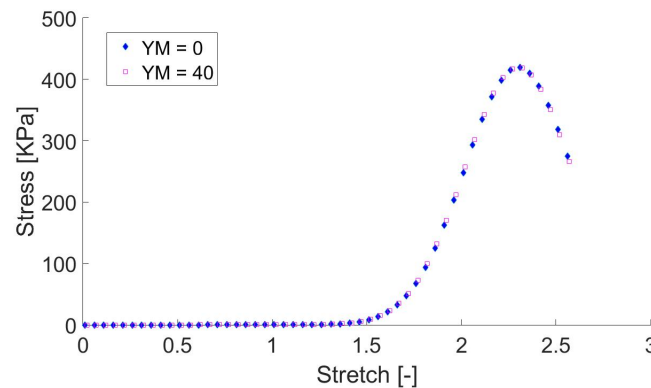


Figure 6.15: Influence of the YM on the predicted uniaxial tensile tests. Both samples have $NVB = 3$ and $Age = 63.6$.

Figure 6.15 illustrates how the curves vary with menopause. Just by visualizing the graph, we can see that even when comparing distant values, they are almost overlapping. The difference in the curves constants does not even reach the 2%. Hence this co-variable show a minimal influence on the results. A possible cause for this outcome is the correlation that exists between the menopause and age. Possible, the model did not give relevance to menopause because the age already adds a similar information. However, in average using Menopause produced better results than without it.

Figure 6.16 presents the relation between NVB and the estimated Gauss equation. It is clear that this co-variable has a relevant influence on the curve. It is expressed two examples with different values of NVB. One its value is 0 and the other is 5. The parameter $C1$ value goes from 419 to 456, meaning a variation around 8%. So we can infer that number of vaginal births increases the maximum stress of the uniaxial tensile test. The others parameters do not have significant changes in their values.

It is very relevant to discuss the significance of the co-variables expressed in the previous figures. The

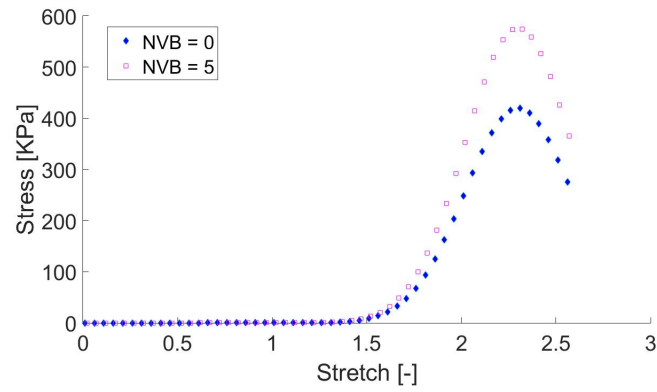


Figure 6.16: Influence of the NVB on the predicted uniaxial tensile tests. Both samples have $YM = 15.5$ and $Age = 63.6$.

model equations provide an excellent base to conclude which ones affect the tests made. Age and NVB are the individual characteristics that have the most prominent relevance. Mainly, they influence the curves' maximum stress. In average, older women and with more children by natural childbirth have higher maximum stress. The other parameters of the Gauss equation appear to do not be affected by them.

Chapter 7

Conclusions

Following an increasing interest in the POP disorder, this thesis investigated the connection between patients characteristics and their vaginal tissues' mechanical properties. The possibility of describing the uniaxial tensile tests applying NLME models was proposed and tested. In this scope, we developed a new approach to describe the dataset using the referred model and to exclude samples considered as being outliers.

We worked on a dataset composed of numerous patients, each one containing several test results. In a first approach, this study tried to approximate the tests observations to a Gauss equation. The fittings results of each sample individually were very accurate, since their RMSE was low. When the process was performed to the data grouped per patient, the errors substantially increased due to the high intra-individual variability. Across this thesis, several patients were presented as examples of the inconstancy of samples that were supposed to be correlated.

A NLME model assumes that there is an association between the individual co-variables and the parameters of the $f(.)$ function. After we performed the fittings, we analyzed the results and concluded that not all co-variables have the same influence on the parameters. The most relevant characteristics are the age and the number of natural childbirths. The existence of hormonal therapy, menopause and the number of pregnancies did not show signs of being significant in the tests results. Several experiences recurring to different functions were performed until we concluded that, in a mathematical form, this correlation is better described with a polynomial equation.

The model success is mainly controlled by the information that we use as an input. When the model was implemented, it was clear that some samples diverged from the patient's general pattern. To surpass this difficulties we developed an iterative process to identify and exclude samples supposed to be outliers. Resorting to the model's random effects estimation, we establish an indicator that quantifies the "worst" tests. This method was applied to several artificial datasets and had excellent results. When it was exposed to noise in the samples, its ability to detect outliers was increased. This outcome is especially interesting because it means that the algorithm handles very well with intra-individual variability. In real datasets, there is a high probability of having outliers resulting from experimental errors. Therefore, this innovative approach can be very useful to clean the data and improve the model accuracy. Another

result worth mention is its robustness to the increasing number of outliers in the dataset. In the worst scenario, we introduced 20% of outliers, and the algorithm was still capable of excluding the outliers. Then, the iterative process was applied to real data to verify its ability to improve the model accuracy. The overall results confirmed the evidence shown in the previous trials. The removal of 15 samples reduced the variance of the random effects more than 40%. The error also was improved, dropping around 10%. We should emphasize that we were conservative in deciding the number of samples to be removed. If more tests were excluded, the results improvement would be more significant.

Concerning the primary purpose of this thesis, we concluded that there is some evidence that suggests that patient is associated with the mechanical properties of vaginal tissues. The final model's equations support the theory that age and number of natural childbirths actively affect the maximum stress observed in the tests. Following the results obtained, we can speculate that when the women get older, their vaginal tissues reach higher values of stress during the tests, although we cannot infer that from this type of cross-sectional study. The same applies to the number of normal childbirths.

Although the trends observed, the model did not describe the data with the precision expected due to various constraints. The number of samples was proved to be insufficient to achieve better results. Aware of the need to estimate several parameters, this factor was the main limitation of this thesis. Since in the require estimations, we need a statistically significant number of samples to avoid over-fitting problems. Considering that we only used 87 observations, it is very challenging to implement one model with the complexity required to describe the dynamics present in the system. Another restriction factor was the high intra-individual variability that distorts the patients' fittings. Numerous samples did not present any signs of correlation with the others from the same patient.

This work planned to extend the developed approach to other fields. In this context, the methods applied were conceived to be easily employed on different datasets. The program applies the iterative process and creates the models semi-automatically. Which means that is very simple to introduce another dataset and create a model from it. One of this thesis's main achievements is the results given by the iterative process. This method has the potential to be implemented in every system described by a NLME model as a valuable tool to improve their accuracy.

Reviewing the work accomplished, we conclude that this thesis made a few steps to improve the knowledge about the POP disorder. We concluded that some individual characteristics influence the tissues mechanical properties, which can promote the development of diagnosis means and treatments methods.

7.1 Future Work

Throughout this thesis, we discussed the relevance of predicting tissues' mechanical properties. This study achievements help their understanding, but there are many questions that we still do not have an answer. In the future, the NLME models should be applied to different datasets of mechanical tests on tissue to perceive if the results were affected by the quality of our data.

As explained in previous chapters, one of our purposes was to explore the possibility of applying NLME

to other human tissues. This objective was not achieved in the current thesis. Since the literature and our results support that opportunity, we believe that could produce significant outcomes in other fields of interest.

Finally, we consider that applying the iterative process in other application can be proved to be very useful. This method was developed to do not be restricted to our dataset. Therefore, applying it to another context is relatively easy to perform and has the potential to improve the results considerably. This approach is entirely innovative, so there are many areas of interest to apply the algorithm.

Bibliography

- [1] V. Svihrova, J. Svihra, J. Luptak, S. Swift, and G. Digesu. Disability-adjusted life years (dalys) in general population with pelvic organ prolapse: a study based on the prolapse quality-of-life questionnaire (p-qol). *European Journal of Obstetrics Gynecology and Reproductive Biology*, 2014.
- [2] Nuria L. Mias, Eva M. Franco, Jaume Aguado, and Emilia Sánchez. Pelvic organ prolapse and stress urinary incontinence, do they share the same risk factors. *European Journal of Obstetrics Gynecology and Reproductive Biology*, 2015.
- [3] Sarka Lisonkova, Jessica A. Lavery, Cande V. Ananth, Innie Chen, Giulia Muraca, Geoffrey W. Cundiff, and K. S. Joseph. Temporal trends in obstetric trauma and inpatient surgery for pelvic organ prolapse: an age-period-cohort analysis. *American Journal of Obstetrics and Gynecology*, 2016.
- [4] Marijke C. Ph. Slieker ten Hove, Annelies L. Pool-Goudzwaard, Marinus J. C. Eijkemans, Regine P. M. Steegers-Theunissen, Curt W. Burger, and Mark E. Vierhout. Symptomatic pelvic organ prolapse and possible risk factors in a general population. *American Journal of Obstetrics and Gynecology*, 2009.
- [5] J Eric Jelovsek, Christopher Maher, and Matthew D Barber. Pelvic organ prolapse. *Lancet*, 2007.
- [6] Chrystèle Rubod, Malik Boukerrou, Mathias Brieu, Patrick Dubois, and Michel Cosson. Biomechanical properties of vaginal tissue. part 1: New experimental protocol. *The journal of urology*, 2007.
- [7] C.M. Kim, M.J. Jeon, D.J. Chung, S.K. Kim, J.W. Kim, and S.W. Bai. Risk factors for pelvic organ prolapse. *International Journal of Gynecology and Obstetrics*, 2007.
- [8] E. Peña, P. Martins, T. Mascarenhas, R.M. Natal Jorge, A. Ferreira, M. Doblaréa, and B. Calvo. Mechanical characterization of the softening behavior of human vaginal tissue. *Journal of the Mechanical Behavior of Biomedical Materials*, 2010.
- [9] Shunaha Kim, Marie-Andree Harvey, and Shawna Johnston. A review of the epidemiology and pathophysiology of pelvic floor dysfunction: Do racial differences matter? *Journal of Obstetrics and Gynaecology Canada*, 2005.

- [10] Asa Leijonhufvud, Cecilia Lundholm, Sven Cnattingius, Fredrik Granath, Ellika Andolf, and Daniel Altman. Risks of stress urinary incontinence and pelvic organ prolapse surgery in relation to mode of childbirth. *American Journal of Obstetrics and Gynecology*, 2011.
- [11] Pamela A. Moalli, Soyna Jones Ivy, Leslie A. Meyn, and Halina M. Zyczynski. Risk factors associated with pelvic floor disorders in women undergoing surgical repair. *The American College of Obstetricians and Gynecologists*, 2003.
- [12] Maria Andrada Hamer and Jan Persson. Familial predisposition to pelvic floor dysfunction: prolapse and incontinence surgery among family members and its relationship with age or parity in a swedish population. *European Journal of Obstetrics and Gynecology and Reproductive Biology*, 2013.
- [13] Mulhall, J.P., Incrocci, L., Goldstein, I., and R. Rosen. *Cancer and Sexual Health*. Humana Press, 2011.
- [14] H. Konar. *DC Dutta's Textbook of Gynecology*. Jaypee Brothers, Medical Publishers Pvt. Limited, 2014. ISBN 9789351520689. URL <https://books.google.pt/books?id=40yVAwAAQBAJ>.
- [15] L. Wylie. *Essential Anatomy and Physiology in Maternity Care*. Elsevier, Churchill Livingstone, 2005. ISBN 9780443100413. URL <https://books.google.pt/books?id=Qgp0vSDxGGYC>.
- [16] Anne M. Weber and Mark D. Walters. Anterior vaginal prolapse: Review of anatomy and techniques of surgical repair. *Elsevier Science Inc.*, 1997.
- [17] Jie-Mei Hu, Xiao Cheng, Lin Wang, Jie-Ning Zhu, and Li-Hua Zhou. Vasoactive intestinal peptide expression in the vaginal anterior wall of patients with pelvic organ prolapse. *Taiwanese Journal of Obstetrics and Gynecology*, 2013.
- [18] L. Brown. *Pathology of the Vulva and Vagina*. Essentials of Diagnostic Gynecological Pathology. Springer London, 2012. ISBN 9780857297570. URL <https://books.google.pt/books?id=Yv2CMHoVR9wC>.
- [19] Pedro Martins, Agnaldo Lopes Silva-Filho, Andrea Moura Rodrigues Maciel da Fonseca, Agostinho Santos, Liliana Santos, Teresa Mascarenhas, Renato M. Natal Jorge, and António J. M. Ferreira. Biomechanical properties of vaginal tissue in women with pelvic organ prolapse. *Gynecol Obstet Invest*, 2012.
- [20] Pedro Alexandre Lopes de Sousa Martins. Experimental and numerical studies of soft biological tissues. Master's thesis, Faculdade de Engenharia Universidade do Porto, 2010.
- [21] V. Alastrue, J.F. Rodriguez, B. Calvo, and M. Doblare. Structural damage models for fibrous biological soft tissues. *Gynecol Obstet Invest*, 2006.
- [22] Marko Vulic, Tomislav Strinic, Snjezana Tomic, Vesna Capkun, Ivana Alujevic Jakus, and Stipic Ivica. Difference in expression of collagen type i and matrix metalloproteinase-1 in uterosacral ligaments of women with and without pelvic organ prolapse. *European Journal of Obstetrics and Gynecology and Reproductive Biology*, 2010.

- [23] Lu Zhou, Jung Han Lee, Yan Wen, Christos Constantinou, Murayama Yoshinobu, Sadao Omata, and Bertha Chen. Biomechanical properties and associated collagen composition in vaginal tissue of women with pelvic organ prolapse. *The journal of urology*, 2012.
- [24] Manon H. Kerkhof, Alejandra M. Ruiz-Zapata, Herman Bril, Maaïke C. G. Bleeker, Jeroen A. M. Belien, Reinout Stoop, and Marco N. Helder. Changes in tissue composition of the vaginal wall of premenopausal women with prolapse. *American Journal of Obstetrics and Gynecology*, 2014.
- [25] Estefanía Peña, Juan A. Peña, and Manuel Doblaré. On the Mullins effect and hysteresis of fibered biological materials: A comparison between continuous and discontinuous damage models. *International Journal of Solids and Structures*, 2009.
- [26] P. Martins, E. Peña, R.M. Natal Jorge, A. Santosd, L. Santosd, T. Mascarenhas, and B. Calvo. Mechanical characterization and constitutive modelling of the damage process in rectus sheath. *Journal of mechanical behavior of biomedical materials*, 2012.
- [27] P. Martins, E. Pena, B. Calvob, M. Doblare, T. Mascarenhas, R. Natal Jorge, and A. Ferreira. Prediction of nonlinear elastic behaviour of vaginal tissue: experimental results and model formulation. *Computer Methods in Biomechanics and Biomedical Engineering*, 2010.
- [28] B. Calvo, E. Pena, P. Martins, T. Mascarenhas, M. Doblare, R.M. Natal Jorge, and A. Ferreira. On modelling damage process in vaginal tissue. *Journal of Biomechanics*, 2009.
- [29] Christoffer W.T Ornoea, Henrik Agerso, E.Niclas Jonsson, Henrik Madsen, and Henrik A.Nielsen. Non-linear mixed-effects pharmacokinetic pharmacodynamic modelling in nlme using differential equations. *Computer Methods and Programs in Biomedicine*, 2004.
- [30] Victor H. Lachos, Luis M. Castro, and Dipak K. Dey. Bayesian inference in nonlinear mixed-effects models using normal independent distributions. *Computational Statistics and Data Analysis*, 2013.
- [31] J. Antic, C.M. Laffont, D. Chafaï, and D. Concordet. Comparison of nonparametric methods in nonlinear mixed effects models. *Computational Statistics and Data Analysis*, 2009.
- [32] Marek Brabec, Ondřej Konár, Emil Pelikán, and Marek Malý. A nonlinear mixed effects model for the prediction of natural gas consumption by individual customers. *International Journal of Forecasting*, 2008.
- [33] Shawn X. Meng, Shongming Huang, Victor J. Lieffers, Thompson Nunifu, and Yuqing Yang. Wind speed and crown class influence the height–diameter relationship of lodgepole pine: Nonlinear mixed effects modeling. *Forest Ecology and Management*, 2008.
- [34] X. Yuan and M.D. Pandey. A nonlinear mixed-effects model for degradation data obtained from in-service inspections. *Reliability Engineering and System Safety*, 2009.
- [35] Tristan Lorino, Philippe Lepert, Jean-Marie Marion, and Hussein Khraibani. Modeling the road degradation process: non-linear mixed effects for correlation and heteroscedasticity of pavement longitudinal data. *Procedia - Social and Behavioral Sciences*, 2012.

- [36] Jeremy Burdona, Patrick Connolly, Nihal de Silva, Nagin Lallu, Jonathan Dixonb, and Henry Pak-baThe. A meta-analysis using a logit non-linear mixed effects model for 'hass' avocado postharvest performance data. *Postharvest Biology and Technology*, 2013.
- [37] Marie DAVIDIAN and David M. GILTINAN. Nonlinear models for repeated measurement data: An overview and update. *Journal of Agricultural, Biological, and Environmental Statistics*, 2003.
- [38] H.B. Motra, J. Hildebrand, and A. Dimmig-Osburg. Assessment of strain measurement techniques to characterise mechanical properties of structural steel. *Engineering Science and Technology, an International Journal*, 2014.
- [39] Hyejeong Janga, Daniel J. Conklin, and Maiying Kong. Piecewise nonlinear mixed-effects models for modeling cardiac function and assessing treatment effects. *Computer methods and programs in biomedicine*, 2013.
- [40] John F. Magnotti and Nedret Billor. Finding multivariate outliers in fmri time-series data. *Computers in Biology and Medicine*, 2014.
- [41] Francesco Battaglia. Finding multivariate outliers in fmri time-series data. *Statistics and Probability Letters*, 2005.
- [42] Aurea Grane and Helena Veiga. Wavelet-based detection of outliers in financial time series. *Computational Statistics and Data Analysis*, 2010.
- [43] A.J.Q. Sarnaglia, V.A. Reisen, and C. Lévy-Leduc. Robust estimation of periodic autoregressive processes in the presence of additive outliers. *Journal of Multivariate Analysis*, 2010.
- [44] Domenico Cucina, Antonietta di Salvatore, and Mattheos K. Protopapas. Outliers detection in multivariate time series using genetic algorithms. *Chemometrics and Intelligent Laboratory Systems*, 2014.
- [45] Milos Hauskrecht, Iyad Batal, Michal Valko, Shyam Visweswaran, Gregory F. Cooper, and Gilles Clermont. Robust estimation of periodic autoregressive processes in the presence of additive outliers. *Journal of Biomedical Informatics*, 2013.
- [46] Miao Cui, Kai Yang, Xiao liang Xu, Sheng dong Wang, and Xiao wei Gao. A modified levenberg-marquardt algorithm for simultaneous estimation of multi-parameters of boundary heat flux by solving transient nonlinear inverse heat conduction problems cardiac function and assessing treatment effects. *International Journal of Heat and Mass Transfer*, 2016.
- [47] Zhang Xian and A. Awotunde. Improvement of levenberg-marquardt algorithm during history fitting for reservoir simulation. *PETROLEUM EXPLORATION AND DEVELOPMENT*, 2016.

Appendix A

Results tables

Table A.1: Sample properties

Sample	Max Stress [Mpa]	Stretch at Max Stress [-]	Thickness [mm]	Length [mm]	width [mm]
17_01	239,99	1,65	2,61	14,99	12,93
17_02	758,53	1,82	1,09	15,93	10,35
17_03	280,75	1,58	2,61	23,22	17,48
17_04	436,70	1,53	1,51	16,81	11,38
17_05	442,42	1,51	1,57	15,52	10,35
17_06	181,15	1,80	3,22	13,73	15,76
18_01	825,54	2,01	1,28	10,08	7,68
18_02	649,40	2,05	1,79	10,96	8,57
18_03	609,92	1,94	2,11	11,86	11,62
19_01	191,89	1,56	2,23	13,84	11,20
19_02	858,82	1,69	1,27	15,50	6,93
19_03	792,22	2,17	1,46	10,12	8,10
19_04	675,77	1,71	1,52	11,87	7,26
19_05	375,80	1,86	1,33	12,53	8,25
19_06	485,47	1,65	1,22	13,00	8,01
20_01	314,01	1,91	1,82	13,10	5,53
20_02	603,04	2,14	1,61	12,28	7,51
20_03	241,25	1,87	1,82	13,80	7,59
20_04	1171,69	2,21	1,18	11,04	6,90
20_05	481,17	1,85	1,53	11,59	8,19
20_06	459,94	1,93	1,82	10,57	12,96
23_01	636,92	1,90	0,95	10,68	6,64
23_02	272,68	2,18	1,51	8,75	10,00

Table A.1: Sample properties

Sample	Max Stress [Mpa]	Stretch at Max Stress [-]	Thickness [mm]	Length [mm]	width [mm]
23_03	302,77	1,92	1,46	12,62	7,01
23_04	200,26	2,65	1,73	8,37	6,06
24_01	420,31	1,69	1,07	8,75	5,95
24_02	448,17	1,65	1,18	8,07	5,17
24_03	778,87	1,84	0,68	6,53	4,21
25_01	326,30	1,97	1,18	7,67	7,34
25_02	376,60	2,02	0,86	9,44	5,40
25_03	589,37	1,76	0,86	6,75	5,40
25_04	423,22	1,59	1,03	9,44	6,75
26_01	576,77	1,85	1,18	6,61	7,71
26_02	447,08	1,59	1,18	8,21	9,06
26_03	414,67	1,72	0,90	5,95	7,36
26_04	1206,28	1,93	1,39	6,29	10,29
26_05	242,98	2,08	1,82	4,62	10,68
26_06	1419,90	2,59	1,18	5,15	13,43
27_01	317,33	1,69	1,87	13,40	3,02
27_02	309,05	1,81	2,53	8,80	13,08
28_01	240,87	2,10	1,50	6,50	8,12
28_02	254,52	1,50	1,50	16,31	5,44
29_01	275,80	1,77	1,91	9,48	8,80
29_02	906,47	1,88	1,16	10,86	6,19
30_01	522,86	1,60	1,16	12,03	7,93
30_02	635,45	1,77	0,93	9,42	7,67
30_03	497,43	1,74	1,02	10,13	4,25
30_04	505,41	2,07	0,90	6,79	6,23
31_01	912,02	2,11	1,40	6,45	10,89
31_02	437,03	2,33	1,61	5,63	9,04
31_03	794,94	1,85	1,25	8,45	8,51
31_04	339,58	1,74	1,29	8,98	8,50
31_05	1565,91	2,73	1,15	5,45	5,86
31_06	1043,88	2,29	1,23	5,64	5,92
32_01	945,34	1,78	1,12	17,86	7,20
32_02	839,98	2,49	1,52	4,84	9,57
33_01	901,24	2,32	1,52	7,21	8,86

Table A.1: Sample properties

Sample	Max Stress [Mpa]	Stretch at Max Stress [-]	Thickness [mm]	Length [mm]	width [mm]
33_02	900,51	1,95	1,24	8,29	10,76
38_01	966,16	1,89	0,97	7,08	7,39
38_02	1046,14	2,09	1,22	5,91	6,52
38_03	818,17	1,76	1,11	7,71	5,71
38_04	1173,10	1,96	0,96	7,09	6,78
49_01	237,34	1,56	1,17	9,96	7,92
49_02	448,24	1,56	1,27	13,10	6,58
50_01	305,12	2,20	1,63	8,49	8,77
51_01	514,31	1,52	1,61	17,52	13,01
51_02	437,41	1,97	2,02	17,74	12,96
52_01	390,74	1,62	1,52	14,58	10,05
52_02	1400,02	2,10	0,95	12,06	11,33
53_01	215,82	1,73	1,59	13,00	9,84
53_02	374,46	2,10	0,92	7,34	10,59
54_01	346,56	2,55	1,36	7,86	11,30
54_02	439,60	2,18	1,30	5,69	7,57
54_03	474,74	2,11	1,10	5,48	7,33
55_01	599,33	1,89	1,30	7,69	6,05
55_02	340,91	2,03	1,80	10,00	6,49
55_03	460,86	2,06	2,15	8,03	8,70
57_01	562,44	2,00	1,37	7,24	6,06
57_02	174,72	1,84	1,59	9,85	7,63
57_03	390,64	1,89	1,41	13,86	9,07
60_01	139,43	2,01	2,04	14,44	7,14
60_02	231,81	1,49	1,60	9,88	5,40
60_03	208,53	1,68	1,02	8,12	5,35
62_01	592,59	1,59	1,85	15,03	7,27
62_02	483,60	1,69	2,35	16,19	8,31
62_03	159,75	1,71	2,25	14,21	9,43
62_04	543,85	2,00	1,81	7,97	9,46
66_01	483,38	1,65	1,22	14,74	6,49
66_02	316,90	1,82	1,78	12,64	6,01

Table A.2: Fittings results of the real data Patients

Patient ID	c_1 [-]	c_2 [-]	c_3 [-]	RMSE [MPa]	R-square [-]
17	515,2769	1,909339	0,447196	90,025	0,701
18	699,9877	2,015483	0,350612	41,042	0,974
19	720,3475	2,001047	0,502022	111,873	0,777
20	1157,772	2,449996	0,602545	79,383	0,887
23	315,3986	1,957076	0,523943	102,883	0,559
24	768,8307	1,927116	0,443886	55,023	0,931
25	349,2163	1,881619	0,48926	97,419	0,617
26	1432,643	2,783902	0,931131	153,561	0,802
27	316,1738	1,7298	0,3059	15,122	0,983
28	235,8059	1,871718	0,57102	54,855	0,664
29	1206,465	2,158002	0,455191	87,559	0,879
30	545,6739	1,832841	0,438283	87,646	0,819
31	1537,879	3,001096	0,969074	127,055	0,864
32	830,4018	2,130377	0,63275	157,792	0,733
33	883,8011	2,161717	0,550551	102,678	0,904
38	1058,841	2,021209	0,448064	66,183	0,965
49	357,7536	1,583295	0,250746	42,636	0,895
50	301,8661	2,23161	0,384464	4,569	0,998
51	644,5881	2,602003	0,886083	111,682	0,487
52	1378,097	2,090233	0,462374	42,461	0,990
53	368,7125	2,103256	0,555894	16,892	0,977
54	382,4788	2,200345	0,628689	49,908	0,890
55	430,0393	1,931508	0,432939	56,176	0,894
57	687,3048	2,305012	0,585231	47,262	0,899
60	153,1704	1,705947	0,437732	36,985	0,698
62	480,6602	1,900537	0,469455	95,805	0,694
66	359,7238	1,671626	0,29532	64,201	0,819

Table A.3: Fittings results of the real data samples

Sample ID	c1 [-]	c2 [-]	c3 [-]	RMSE [MPa]	R-square [-]
17_01	235,488	1,605	0,279	3,805	0,998
17_02	768,209	1,857	0,326	7,286	0,999

Table A.3: Fittings results of the real data samples

Sample ID	c1 [-]	c2 [-]	c3 [-]	RMSE [MPa]	R-square [-]
17_03	276,443	1,598	0,228	3,909	0,998
17_04	438,972	1,560	0,223	5,586	0,999
17_05	441,026	1,524	0,192	4,274	0,999
17_06	179,685	1,754	0,303	2,707	0,998
18_01	825,336	2,021	0,325	5,189	1,000
18_02	645,298	2,007	0,311	7,186	0,999
18_03	597,339	1,934	0,347	6,941	0,999
19_01	192,046	1,498	0,212	3,464	0,998
19_02	869,427	1,734	0,285	12,317	0,998
19_03	772,761	2,063	0,381	10,821	0,999
19_04	666,095	1,669	0,284	8,394	0,999
19_05	358,642	1,802	0,311	4,337	0,999
19_06	477,932	1,619	0,239	3,230	1,000
20_01	304,598	1,845	0,371	6,951	0,997
20_02	607,264	2,020	0,360	10,919	0,998
20_03	239,832	1,833	0,292	1,817	1,000
20_04	1124,340	2,177	0,385	9,764	0,999
20_05	473,800	1,839	0,286	3,318	1,000
20_06	448,969	1,911	0,360	5,267	0,999
23_01	632,148	1,850	0,393	7,014	0,999
23_02	256,796	2,078	0,594	12,387	0,985
23_03	300,702	1,836	0,336	9,485	0,994
23_04	204,107	2,373	0,683	13,510	0,974
24_01	418,210	1,708	0,336	5,268	0,999
24_02	467,980	1,710	0,330	9,034	0,996
24_03	790,907	1,752	0,300	19,807	0,995
25_01	323,921	1,968	0,375	3,207	0,999
25_02	376,763	2,005	0,330	2,374	1,000
25_03	607,934	1,796	0,429	16,149	0,994
25_04	419,184	1,581	0,267	7,200	0,998
26_01	575,060	1,821	0,326	3,354	1,000
26_02	452,847	1,556	0,220	7,981	0,998
26_03	400,607	1,674	0,338	12,070	0,994
26_04	1251,674	2,015	0,462	15,891	0,998

Table A.3: Fittings results of the real data samples

Sample ID	c1 [-]	c2 [-]	c3 [-]	RMSE [MPa]	R-square [-]
26_05	244,593	2,014	0,405	3,310	0,999
26_06	1402,118	2,585	0,639	12,033	0,999
27_01	315,178	1,660	0,245	3,760	0,999
27_02	306,012	1,790	0,349	2,405	1,000
28_01	239,427	2,000	0,438	5,426	0,997
28_02	251,722	1,479	0,230	2,955	0,999
29_01	273,281	1,752	0,281	1,779	1,000
29_02	912,052	1,908	0,321	5,518	1,000
30_01	518,062	1,560	0,239	4,854	0,999
30_02	633,186	1,739	0,375	9,519	0,998
30_03	497,029	1,698	0,264	4,871	0,999
30_04	504,454	1,999	0,359	7,452	0,998
31_01	910,478	2,076	0,393	5,125	1,000
31_02	430,955	2,194	0,549	13,258	0,994
31_03	827,747	1,898	0,275	6,761	0,999
31_04	347,753	1,778	0,294	3,682	0,999
31_05	1615,350	2,857	0,698	18,240	0,999
31_06	1040,057	2,284	0,446	6,636	1,000
32_01	947,265	1,792	0,305	14,472	0,998
32_02	828,686	2,513	0,634	8,159	0,999
33_01	883,763	2,270	0,520	6,789	1,000
33_02	891,037	1,899	0,366	8,175	0,999
38_01	978,443	1,945	0,420	9,543	0,999
38_02	1045,514	2,104	0,427	5,712	1,000
38_03	848,519	1,814	0,332	8,251	0,999
38_04	1191,417	2,020	0,423	9,888	0,999
49_01	238,417	1,551	0,225	2,819	0,999
49_02	466,437	1,615	0,273	5,974	0,998
50_01	326,558	2,284	0,420	4,569	0,998
51_01	529,186	1,556	0,235	5,734	0,999
51_02	452,390	2,016	0,289	6,609	0,998
52_01	384,027	1,603	0,300	4,685	0,999
52_02	1382,016	2,062	0,421	11,819	0,999
53_01	214,389	1,705	0,334	2,075	0,999

Table A.3: Fittings results of the real data samples

Sample ID	c1 [-]	c2 [-]	c3 [-]	RMSE [MPa]	R-square [-]
53_02	370,701	2,063	0,461	5,506	0,998
54_01	333,536	2,369	0,718	12,411	0,991
54_02	430,474	2,165	0,553	4,023	0,999
54_03	464,560	1,998	0,456	5,011	0,999
55_01	593,498	1,852	0,340	4,336	1,000
55_02	323,212	1,932	0,461	9,102	0,995
55_03	451,678	2,008	0,462	5,618	0,999
57_01	569,000	2,010	0,362	6,191	0,999
57_02	171,994	1,797	0,328	2,022	0,999
57_03	374,335	1,868	0,378	6,826	0,998
60_01	126,046	1,896	0,562	18,022	0,879
60_02	237,753	1,510	0,224	4,633	0,997
60_03	209,219	1,630	0,284	3,472	0,998
62_01	578,022	1,571	0,250	9,060	0,998
62_02	485,649	1,682	0,241	5,972	0,999
62_03	158,611	1,695	0,293	1,568	0,999
62_04	530,875	1,985	0,427	6,498	0,999
66_01	478,462	1,653	0,286	5,335	0,999
66_02	311,074	1,807	0,342	3,678	0,999

